Superconducting Nanowire Single Photon Detectors

Gaggero Alessandro
Istituto di Fotonica e Nanotecnologie - IFN-CNR

Why Superconducting Detectors?

Superconducting detectors are the natural choice for very sensitive optical detection:

1- they have small energy gap
2- they work at cryogenic temperatures.

A small energy gap (~1 meV) as compared to semiconductors (~1 eV) implies an absorbed photon produces a much larger number of excitations (no needs to trigger an avalanche)

the inconvenience of operating at cryogenic temperatures (T~4 K) becomes a big advantage in terms of dark count as it is thermally activated

Why Superconducting Nanowires Single Photon Detectors (SNSPD)?

Why superconducting nanowire single photon detector?

- single photon counting from X-ray to MIR
- low dark count rate
- low jitter <100 ps (record 12 ps),
- fast count rates ~GHz;
- Integration in photonic circuits (PICs)

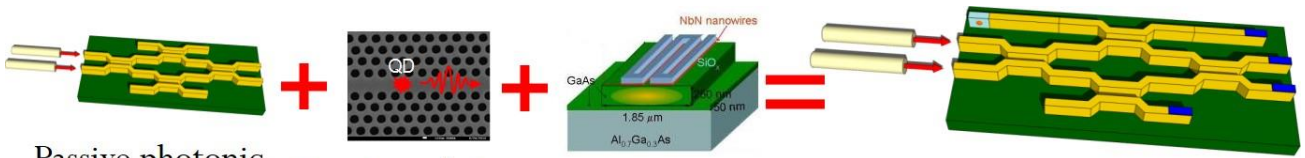

Passive photonic quantum circuits

Quantum dots single photon sources

SNSPDs

SPD technologies VIS-NIR

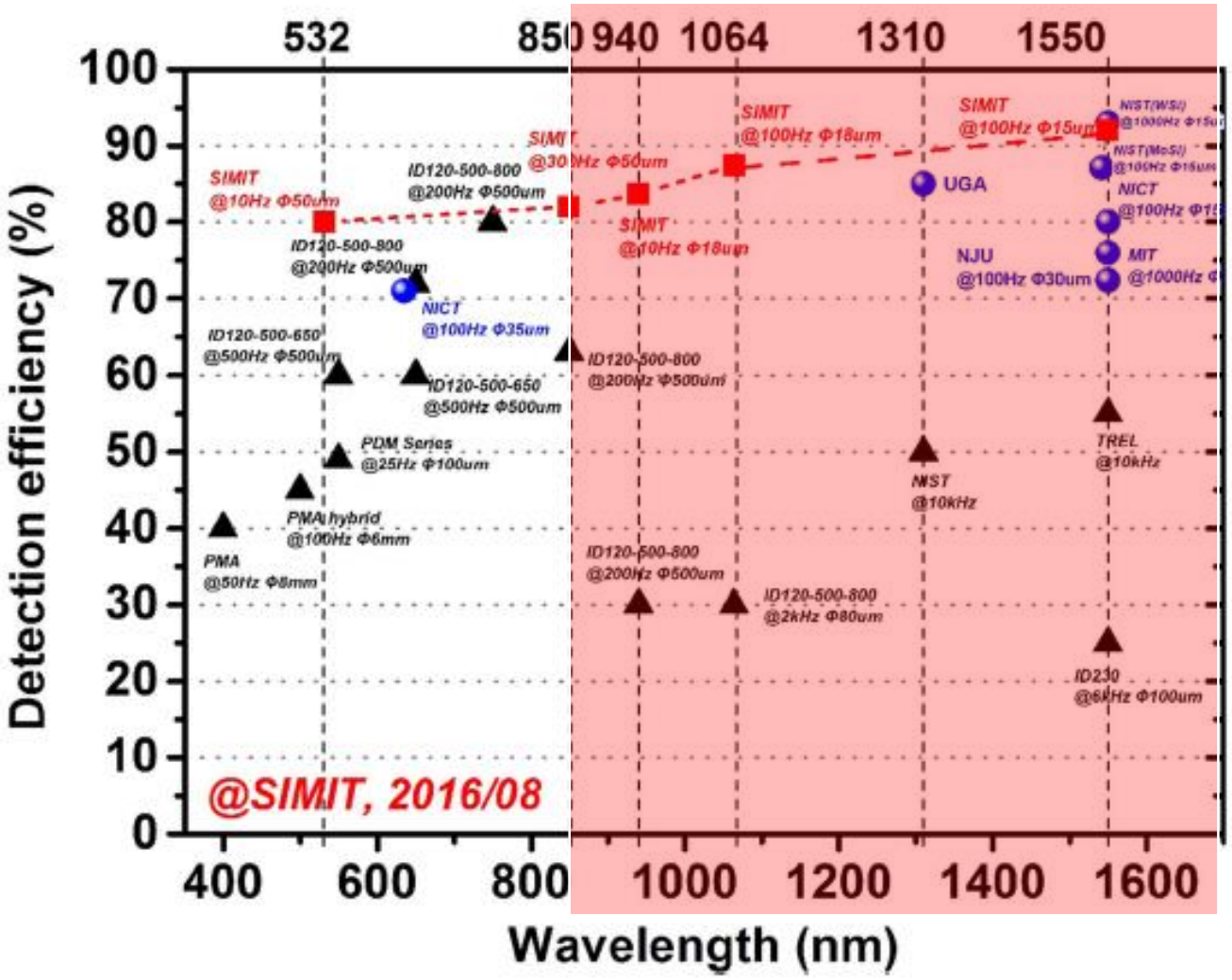

Lixing You et al., SUST (2017)

CNR IFN Istituto di Fotonica e Nanotecnologie

SPD technologies @1550nm

Detector	DE	Maximum count rate	Dark count rate	FWHM Jitter	Operating temp.
PMT	2%	10 MHz	200 kHz	300 ps	200 K
InGaAs APD	10%	100 MHz	16 kHz	55 ps	250 K
TES	95%	100 kHz	< 1Hz	100 ns	0.1K
SNSPD	**93%**	**1GHz (potential)**	**< 10 Hz**	**< 20 ps**	**2.5 K**

$$\text{DE (detection efficiency)} = \frac{\#\ \text{detected photons}}{\#\ \text{incident photons}}$$

H. Terai, et al." in *Optical Fiber Communication Conference*, paper M3G.4 (2018);

SNSPD working principle

2 states: $R_N = 0$;

$R_N \sim 1k\Omega$;

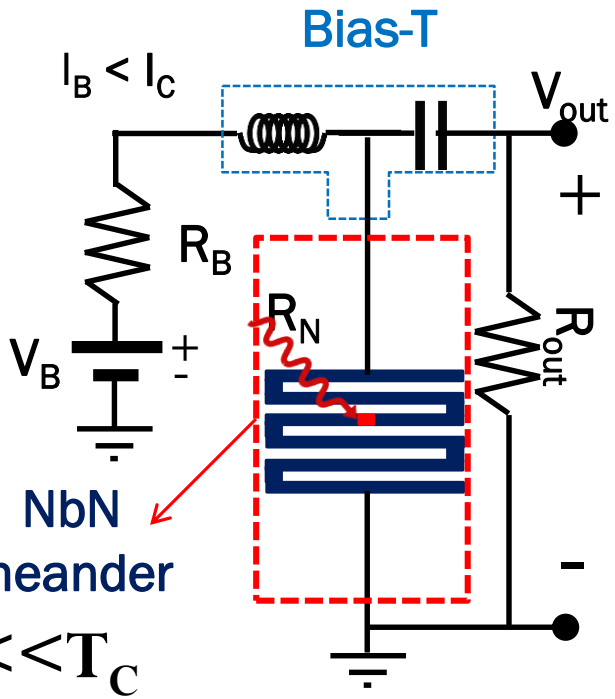

$$V_{out} \approx I_B \times R_{out}$$

$R_{out} = 50\ \Omega$

$$\tau_r = \frac{L_k}{50\ \Omega + R_n}$$

$$\tau_r = \frac{L_k}{50\ \Omega}$$

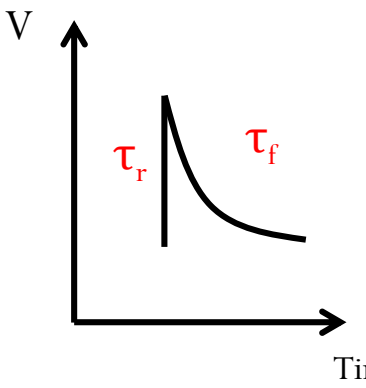

Summary

- Active materials;
- Detection mechanism models;
  (counts vs Darkcounts)
- Detection efficiency;
- Single photon absorption in thin films, DE & SDE;
- Maximum Count rate;
- Timing resolution;
- Integration in photonics circuits (PICS);
- Photon number resolving functionality;
- Multiplexing;

Active materials

Superconductors that have demonstrated capability of single-photon detection are films of compounds or alloys (classified as Type II superconductors):

Polycrystalline films: NbN (niobium nitride), NbTiN (niobium titanium nitride), NbSi, TaN…

Amorphous films: WSi (tungsten silicide) MoSi (Molibdenum Silicide), MoGe (Molybdenum Germanium) etc

Polycrystalline films

NbN, NbTiN Type II superconductors have short ξ.
They can be grown as ultra thin films (with thickness ~ ξ = 3-10 (nm)

$$\xi_0 = \hbar v_F / \pi\Delta$$ Coherence length ~ Cooper pair size

Type I superconductors (λ< ξ)

(Pb, Sn, Al, In)

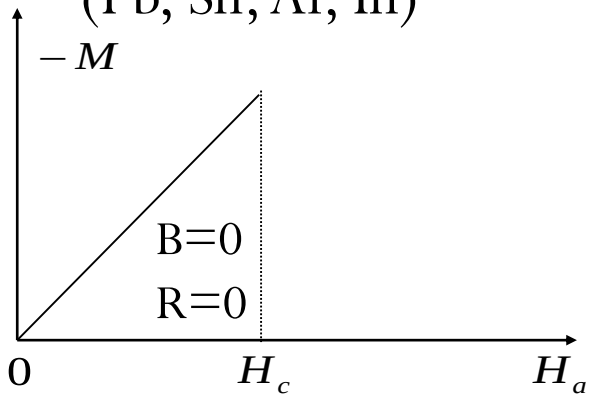

Type I materials: at Hc, abrupt breakdown of the superconductivity

Type II superconductors (λ> ξ)

(alloy and compound)

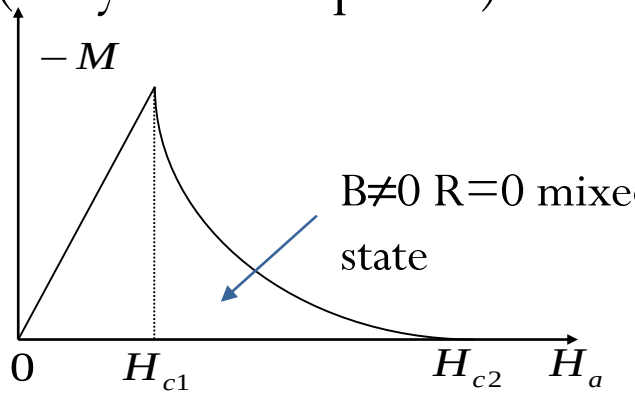

Type II materials: at Hc_1 B begins to penetrate; at Hc_2 total penetration of B

Magnetic Vortices in Type II mixed state

Abrikosov (1957) Nobel Prize 2003

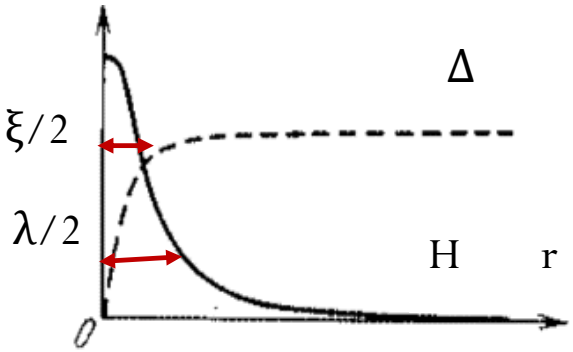

A magnetic vortex has a normal-conducting cylindrical core of radius ~ξ, where a magnetic field persists enclosed by a circular supercurrent surrounded of the superconductive region over a length λ_L .

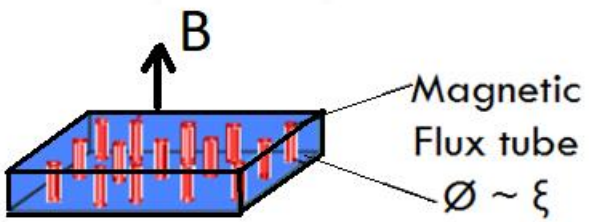

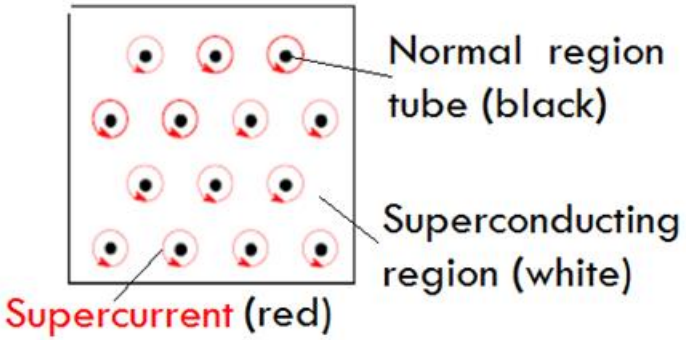

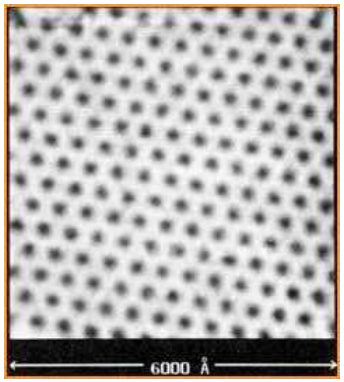

Abrikosov lattice on the surface of NbSe2 film, imaged using STM. In the mixed state the density of vortices increases with *Ha*

Absorption and Quasi Particle Cloud

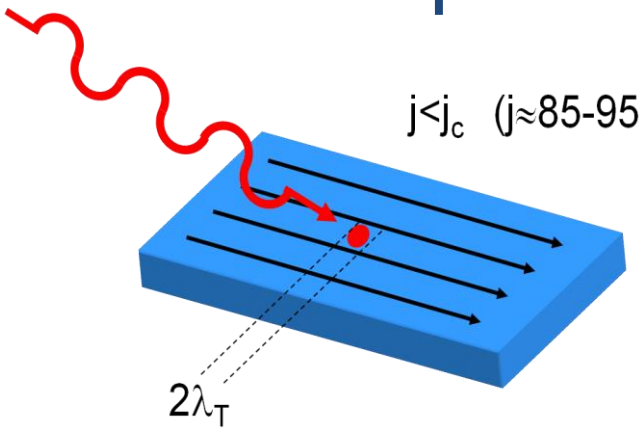

w~100nm wide,
t~4nm thick NbN
Nanowire @T_b~3K

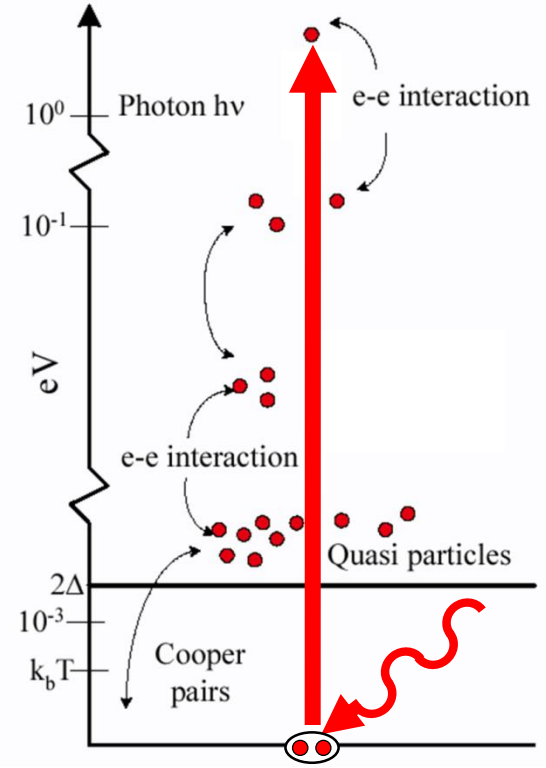

A photon with energy E_{ph} ~ 1eV gets absorbed by breaking a Cooper pair ($E_{ph} >> \Delta$), creating an excited electron

by Goltsman et al., APL (2001)

the hot (excited) electron relaxes, giving rise to a cascading process where several Cooper pairs are broken into excited electrons, creating a cloud of Quasi-Particles (QPs)

Normal-Core Hotspot Model

The QPs cloud diffuses in the nanowire creating **normal-conducting core** (the Hotspot);

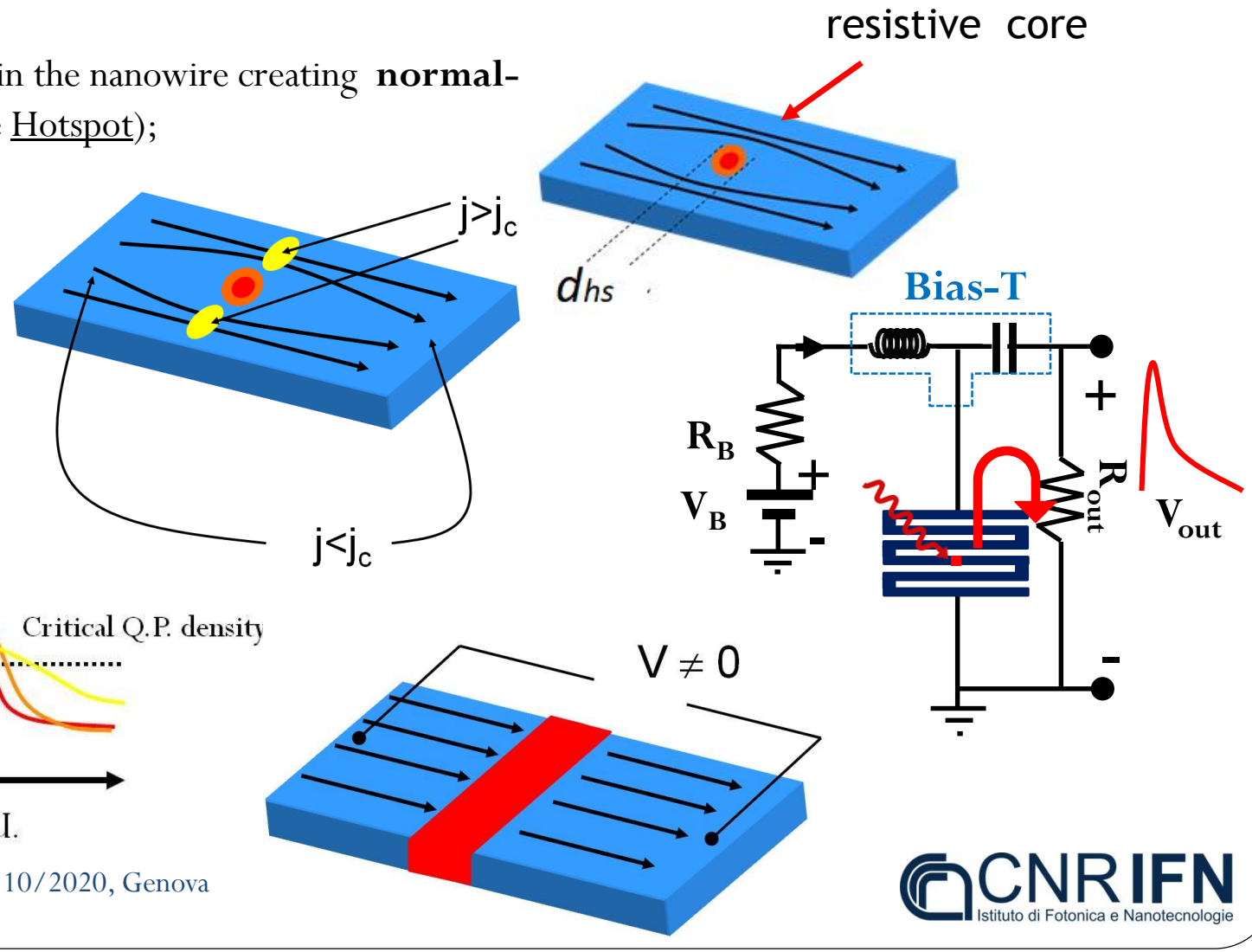

CNR IFN Istituto di Fotonica e Nanotecnologie

Origin of Dark Counts in SNSPDs

Z. Zhou PhD thesis 2014

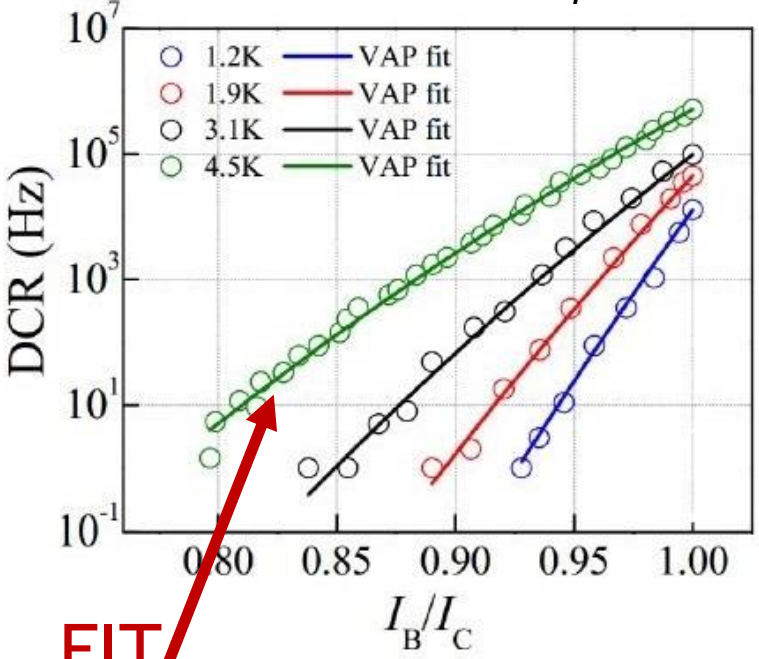

$$P_{VAP} = \Gamma_{VAP}\, e^{-\frac{U_{VAP}}{k_B T}}$$

$$U_{VAP} \propto \Delta$$

Binding VAP potential

Kosterlitz–Thouless (KT) transition, Nobel Prize 2016

- NbN nanowire (thickness ~ξ, width >>ξ) behaves like a 2-D Superconductor.
- Vortex- antivortex pairs (VAP) are pinned in the film (net B=0) below critical temperature T_{KT}

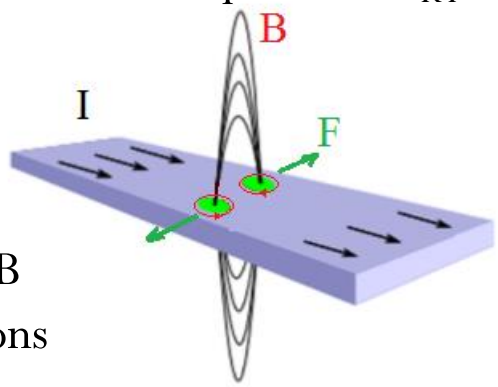

VAP unbinding due to:
- Lorentz force F = I x B
- Temperature fluctuations

Crossing of an unbound vortex (that has a normal core) creates decoherence due to dissipation and then triggers a resistive transition (false pulse => DCR)

Yamashita APL (2011)

Limits of the Normal-Core Hotspot Model

1) The model does not explain origin of dark counts

dark counts due to vortex crossing

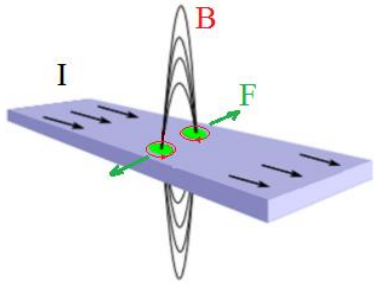

Yamashita APL (2011)

2) The model predicts:

$I_b \sim 1-\alpha\sqrt{E}$

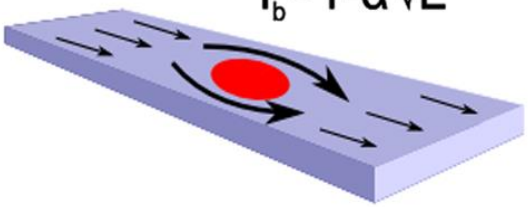

instead

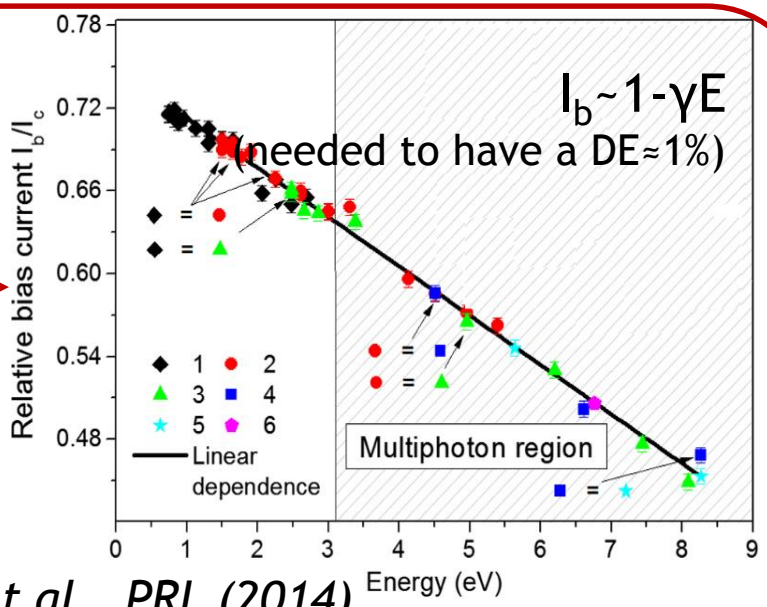

A detection event need $J>J_C$ (close the hotspot), 2i.e. $I_b/I_c > 1 - d_{hs}/w$.

$d_{hs} \sim E^{1/2}$ the hotspot diameter

Renema et al., PRL (2014)

Limits of the Normal-Core Hotspot Model

3) The model predicts a sharp spectral cut-off of the DE with the photon energy.

instead

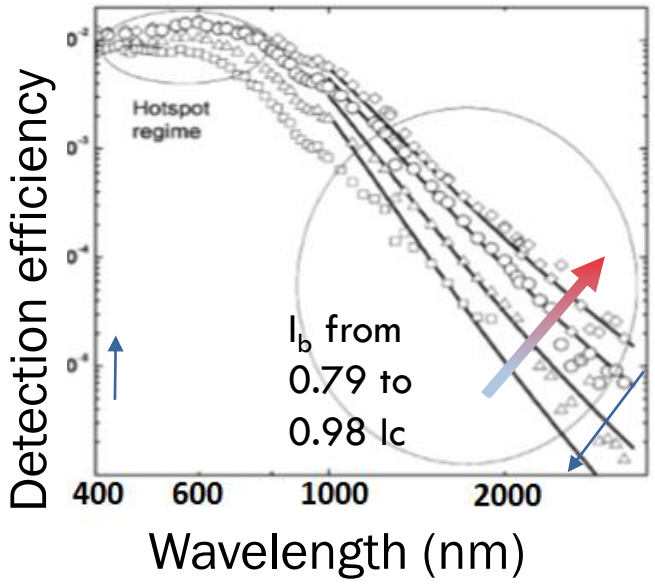

A. Semenov et al 2008

Reason: At low energies the hotspot size to small to trigger the resistive transition

Vortex-crossing model

The cloud of QPs (n_{qp}) diffuse outward from the point of absorption, creating a (red) band of depleted superconductivity with a lower energy gap Δ. This effect stimulates VAP unbinding.

U_{VAP} (Δ) Binding VAP potential

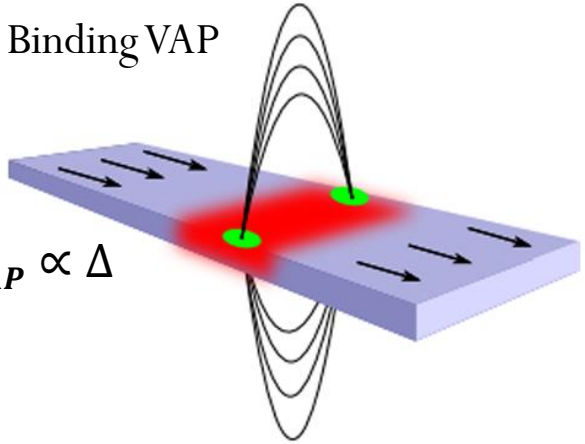

$$U_{VAP} \propto \Delta$$

- A lower Δ decreases U_{VAP} allowing VAP unbinding
- Vortex crossing in the film triggers the resistive transition

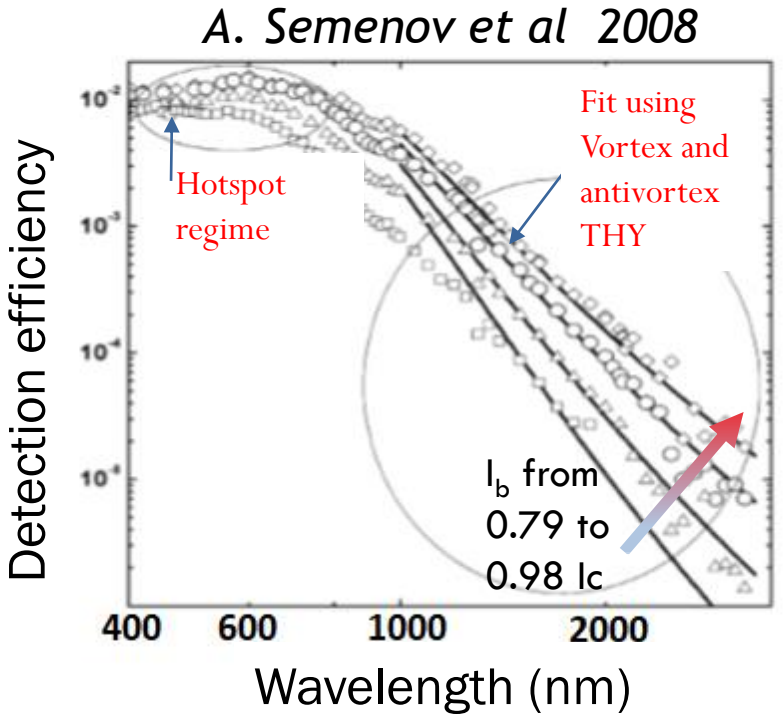

In conclusion, Photon Detection results from the combination of Cooper pair breaking, QP diffusion and Vortex crossing.

- QP diffusion dominates at high energies
- Vortex crossing at low energies

Detection Efficiency

The Detection efficiency (DE) is defined as:

$$DE = \frac{\#\ \text{Counts} - \#\ \text{Dark counts}}{\#\text{incident photons}}$$

DE is a function of the detector bias current $DE(I_B)$.

Measuring DE: single photon regime

μ= average number of photons

n= number of photons

$$P(n) = \frac{e^{-\mu}\,\mu^{n}}{n!}$$

If μ<<1:

$$P(n) = \frac{\mu^{n}}{n!} \quad \Rightarrow \boxed{P(1) = \mu}; \; P(2) \propto \mu^{2}; \; P(3) \propto \mu^{3}$$

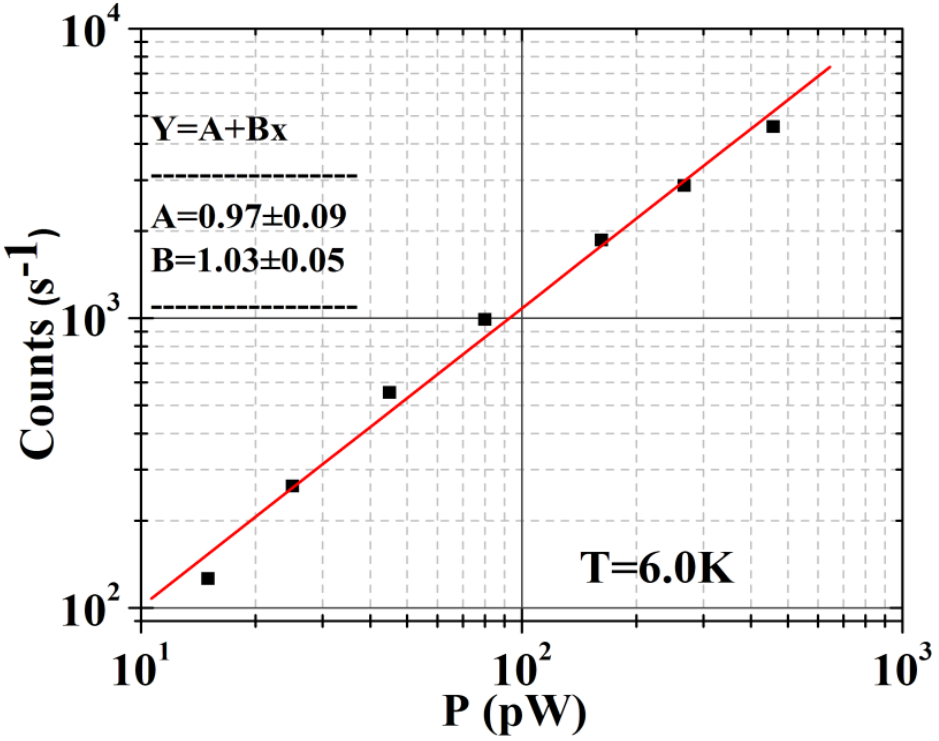

System detection efficiency SDE

$DE = \eta_a \times \eta_i$

$SDE = \eta_C \times \eta_a \times \eta_i$

η_i = internal efficiency;

η_a = probability of absorption

η_C = optical losses in the cryostat;

η_i improved by:

- Homegenity and uniformity of the nanowire;
- Geometry (width, thickness);
- Fabbrication parameters;

η_a improved by

- Single pass cavity
- Integration on waveguide

η_C improved by:

- Meander structuring
- Fiber alignment
- Grating couplers

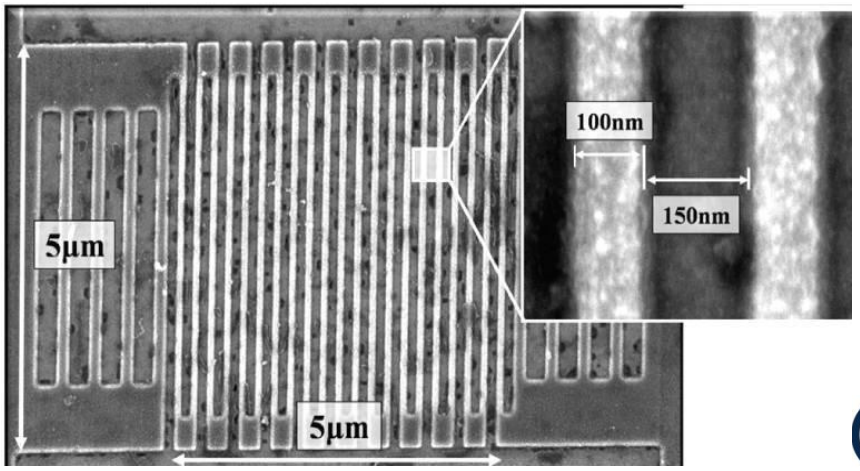

Internal efficiency, η_i

Polycristalline: NbN, NbTiN;
high SNR, low jitter, high repetition rate, low yield

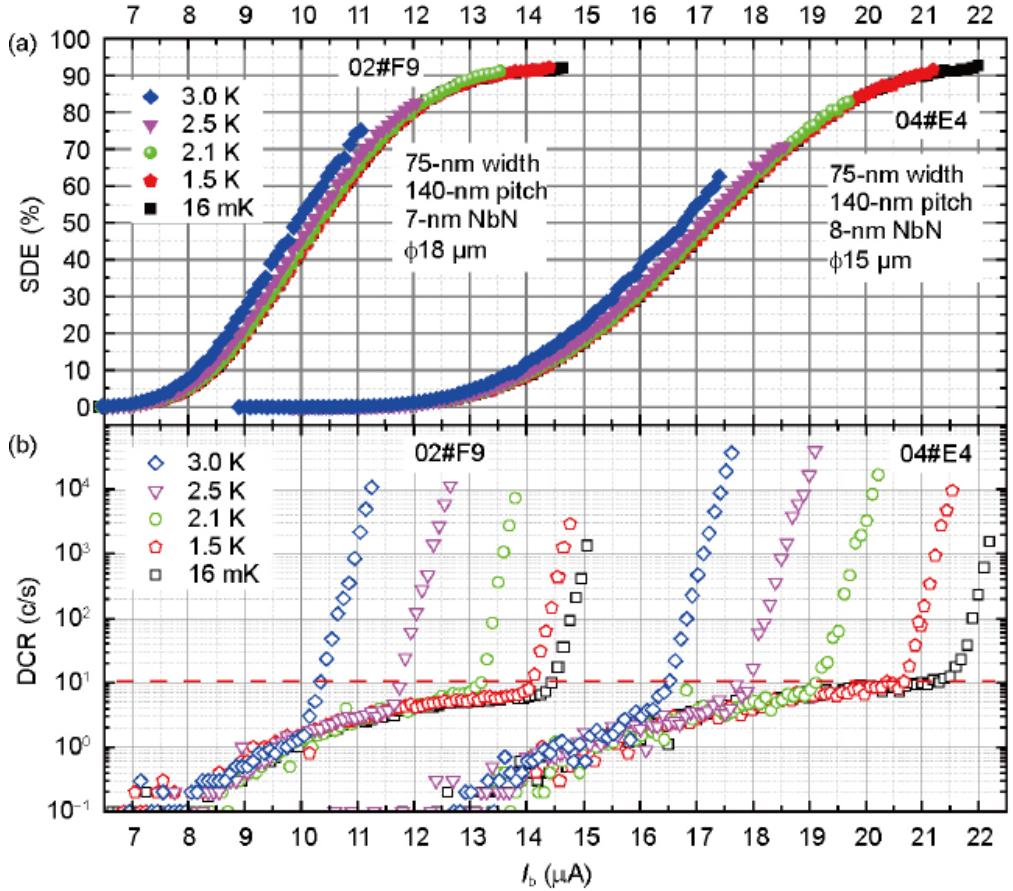

W. J. Zhang et al. Sci. China Phys. Mech. Astron. (2017)

Amorphous: WSi, MoSi;
high SQE, high yield, low SNR, high jitter.

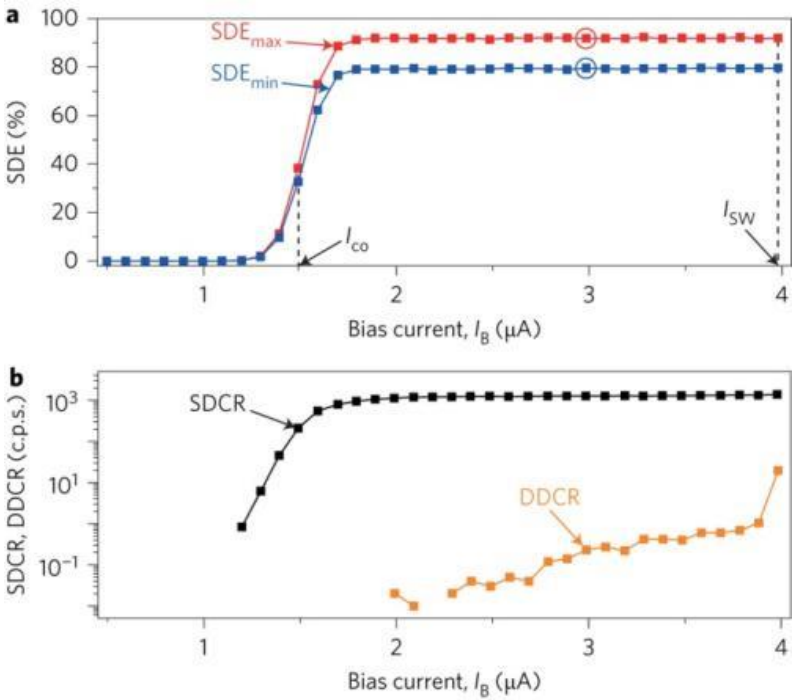

Marsili et al. Nat. Phot (2013);

CNR IFN Istituto di Fotonica e Nanotecnologie

Single photon absorption in Nanowires, η_a

Thin superconducting film (3 nm<d <9 nm), low absorption!

Top coupling

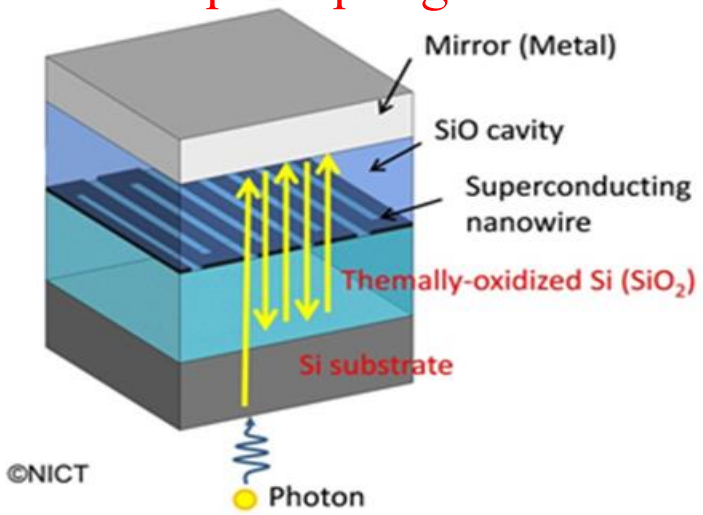

Travelling wave

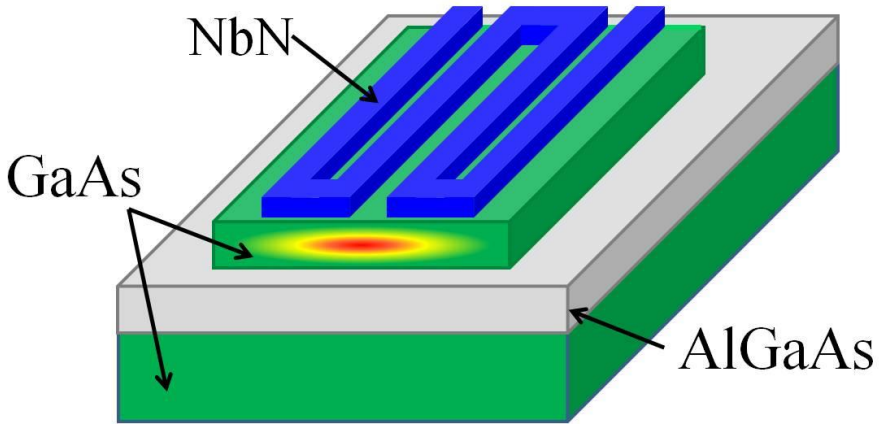

Efficiently Fiber Coupled Detectors

Not Scalable, slower response.

High optical coupling, suitable fiber coupling with external experiments

Integration in photonic circuits

Scalable, faster response, better timing jitter.

High coupling losses, suitable for quantum optics experiments with integrated circuits.

Efficiently Fiber Coupled Detectors:
Absorption in Nanowires, η_a

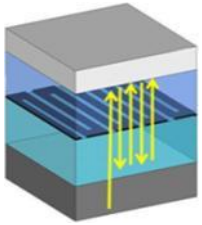

Broad optical cavity:
quarter wavelength mirror

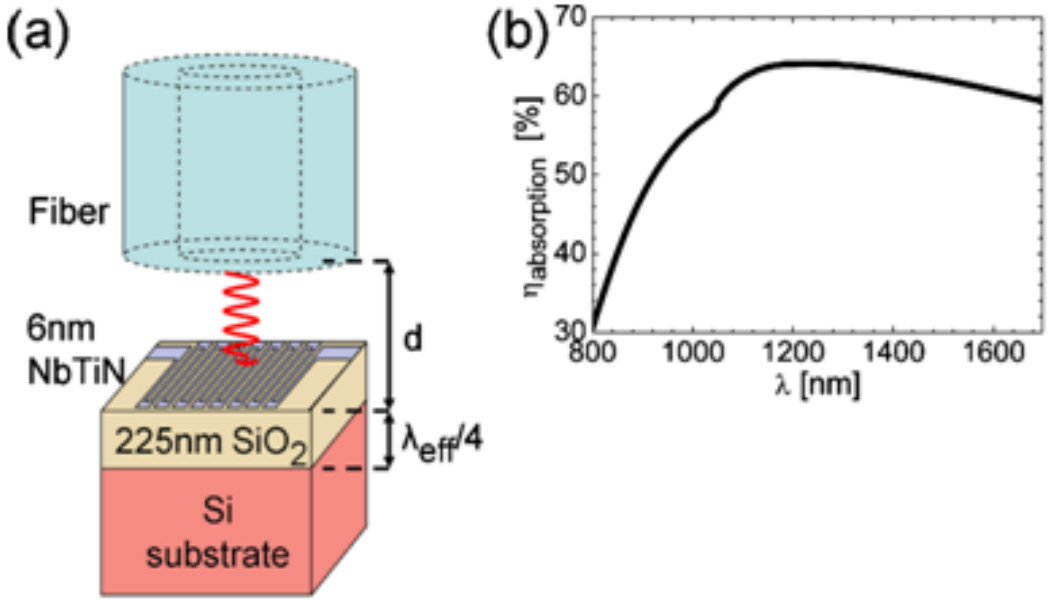

M. G. Tanner et al., *Appl. Phys. Lett.* (2010)

Efficiently Fiber Coupled Detectors:
Absorption in Nanowires, η_a

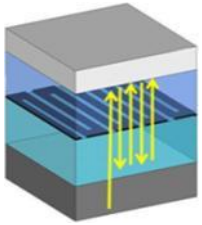

Broad optical cavity:
quarter wavelength mirror

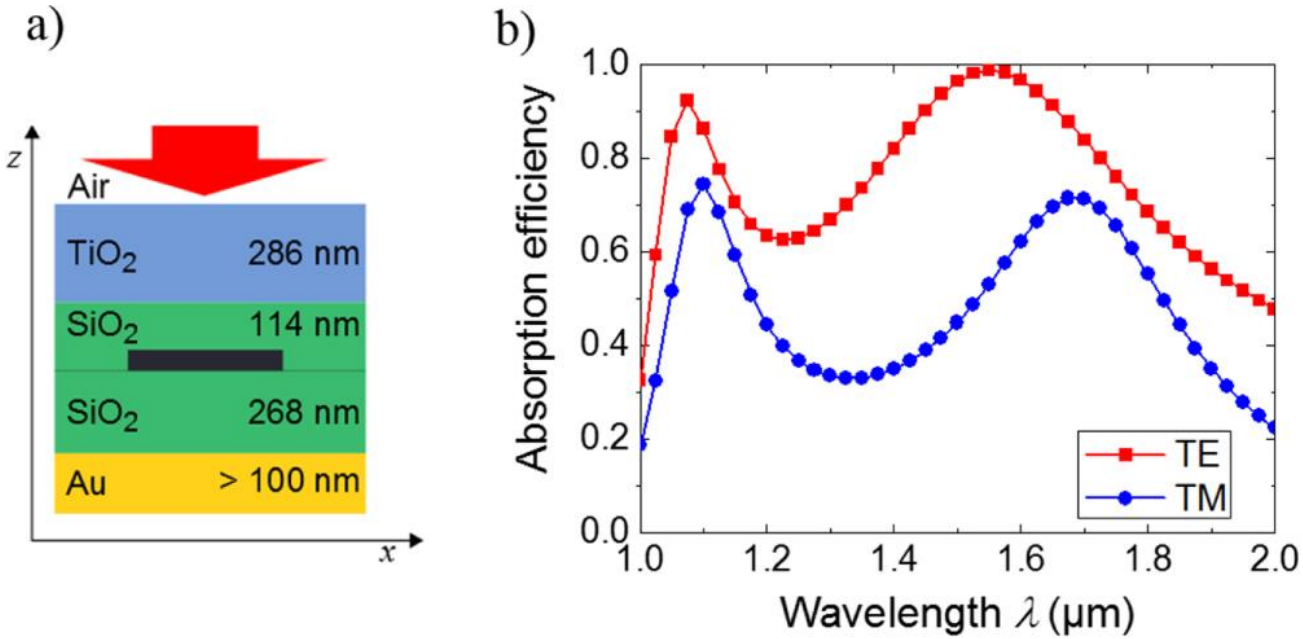

L Redaelli et al., *SUST* (2016)

Efficiently Fiber Coupled Detectors:
Absorption in Nanowires, η_a

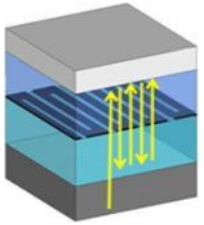

Narrow optical cavity:
distributed bragg reflector

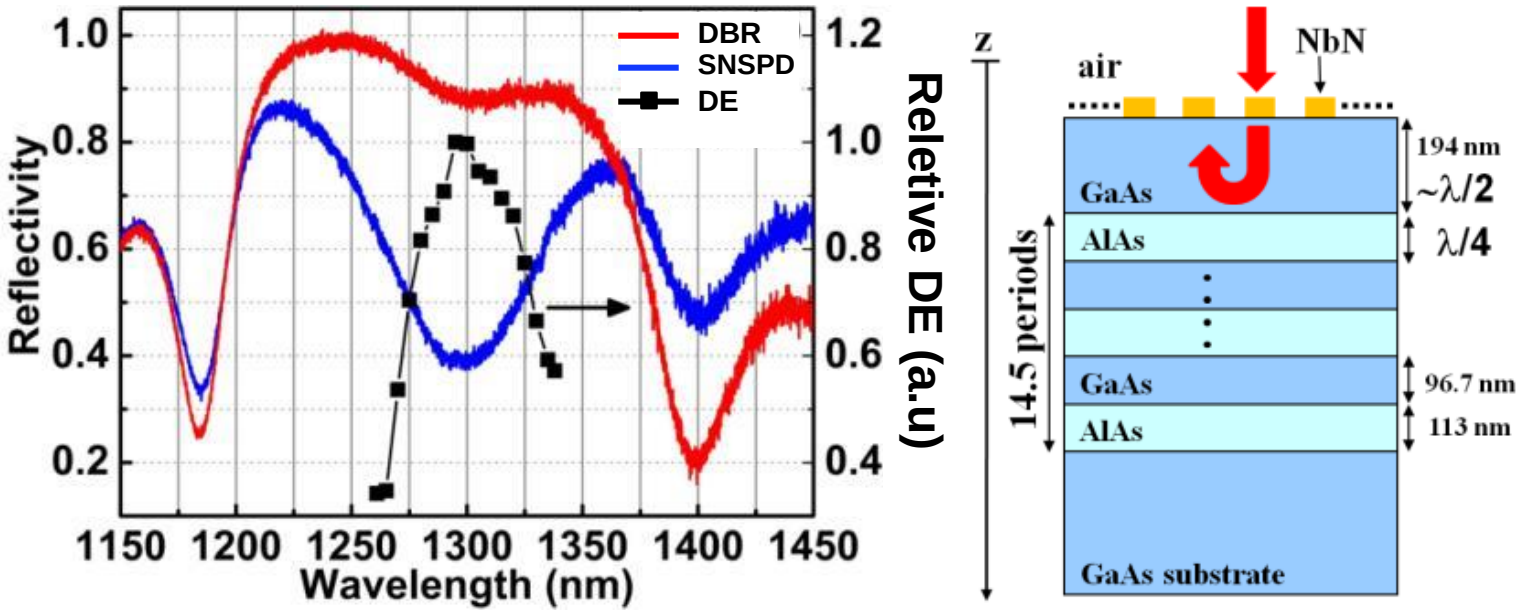

A. Gaggero et al. ,*Applied Physics Letters* (2010)

Maximum Countrate: Hotspot relaxation time (τ_{th})

substrate	t (nm)	w (nm)	s (nm)	I_{sC} (μA)	J_C (MA/cm^2)	τ_{th} (ps)
MgO (100)	5.5	90	110	33	6.7	11.6±0.1
MgF2 (110)	4.5	90	110	22.5	5.4	19.7±0.1
Al2O3 (0001)	7	130	70	21.5	2.4	22.5 ± 0.7
SiO2/Si (100)	7	90	110	21	3.3	22.7 ± 0.1
Si (100)	7.5	90	110	19	2.8	34.5 ± 0.3

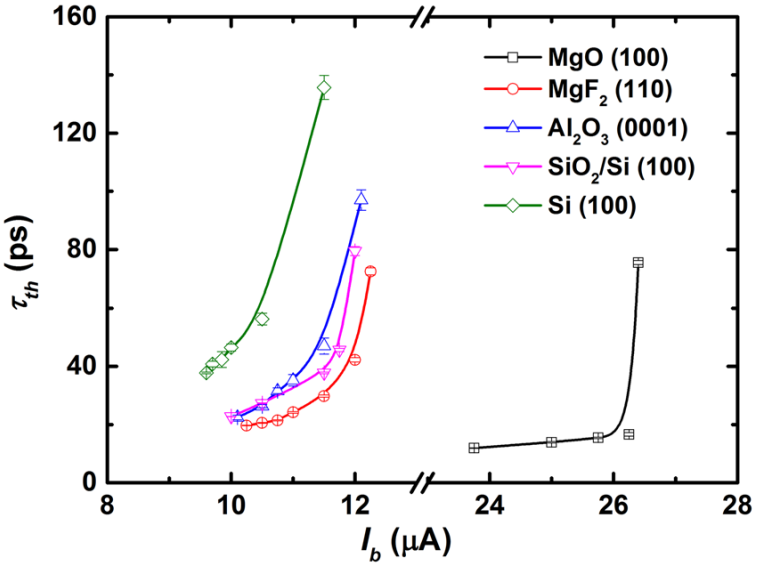

τ_{th} (hotspot relaxation time) depends on film disorder.

τ_{th} physical limit to the maximum countrate achievable

$\tau_{th} \rightarrow$ tens of ps R $\rightarrow$ GHz

Zhang et al. Scientific reports 2018

Maximum Countrate: Kinetic Inductance L_K

In a current-biased superconducting film, after the destruction of a certain number of Cooper pairs, the remaining pairs accelerate to carry the same bias current. Because the pairs are characterized by nonzero inertia, this process can be modelled as time-varying kinetic inductance L_K

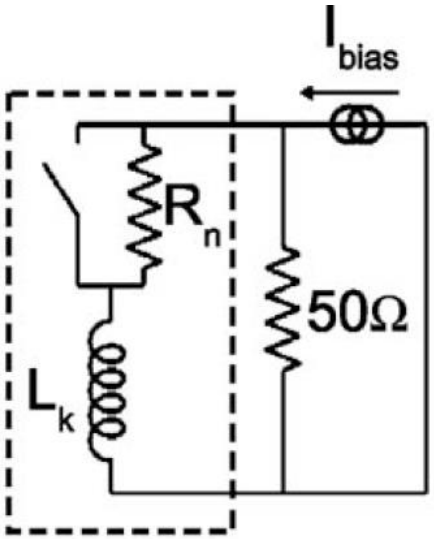

$$L_K = \frac{m}{2n_s e^2}\frac{L}{wd}$$

$$\tau_r = \frac{L_k}{50\ \Omega + R_n} \qquad \tau_f = \frac{L_k}{50\ \Omega}$$

$$\tau_f \rightarrow \text{tens of ns} \quad R \rightarrow \text{MHz}$$

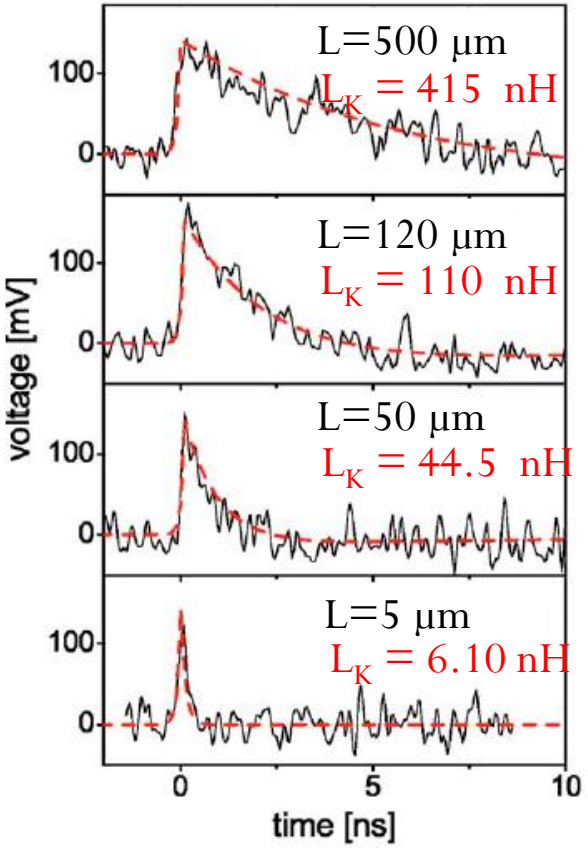

Kerman et al., app phys lett. 2006

Maximum Countrate vs DE

Detector active area diameters Φ = 5, 10, 15, and 18 μm

ϕ (μm)	τ_f (ns)	MCR (MHz)
5	4.8	208
10	11.9	84
15	26.2	38
18	44.4	23

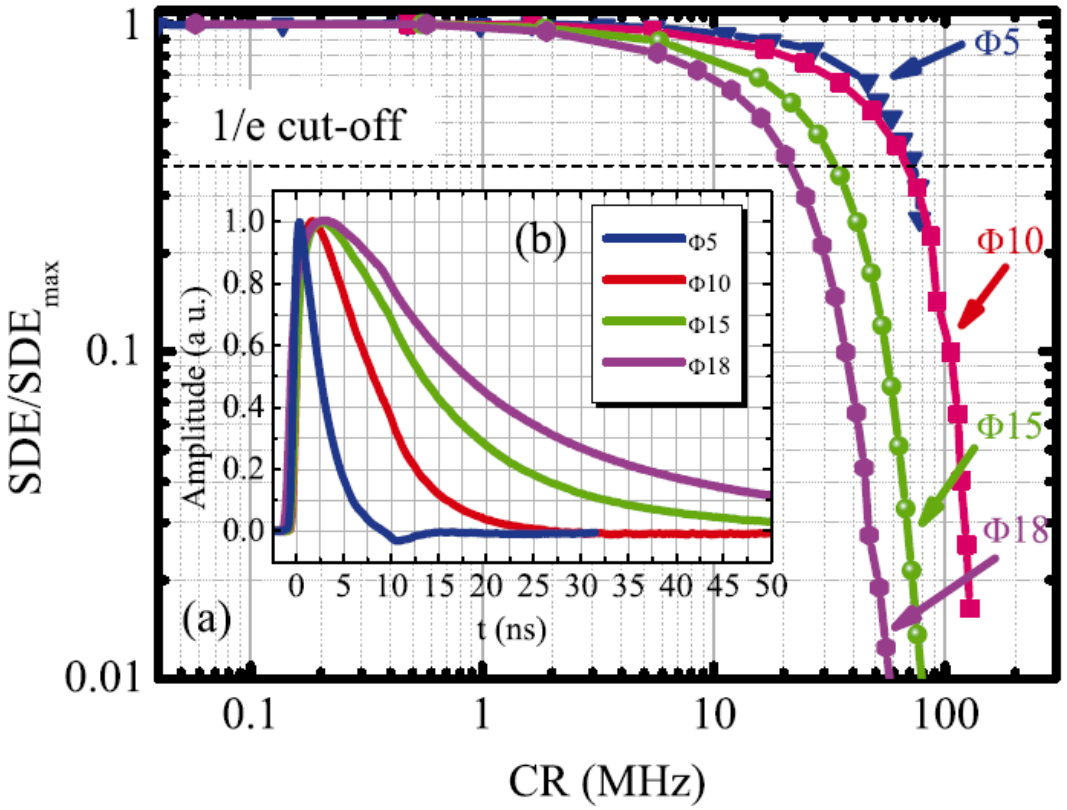

Zhang et al. AIP Advances (2015)

Timing resolution: Jitter

•Timing jitter characterizes the time **delay** between **the detection pulse** and the **the corresponding incident photon**. It is the detector **time resolution**.

•Gaussian distribution and the timing jitter is **FWHM**

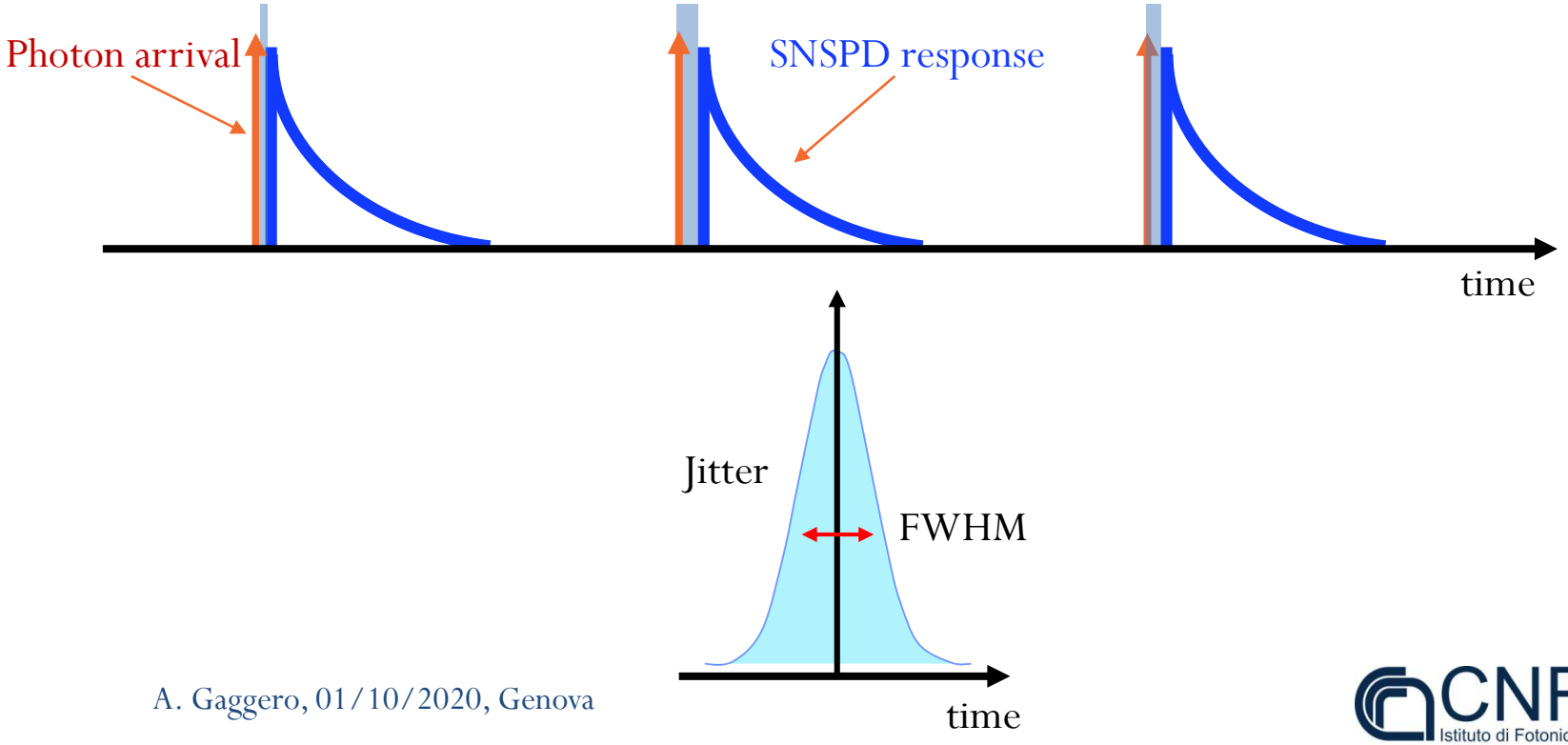

Timing resolution: Jitter

$$J^2_{System} = J^2_{SNR} + \boxed{J^2_{geom} + J^2_{hp}} + J^2_{Setup}$$

$$J^2_{SNSPD}$$

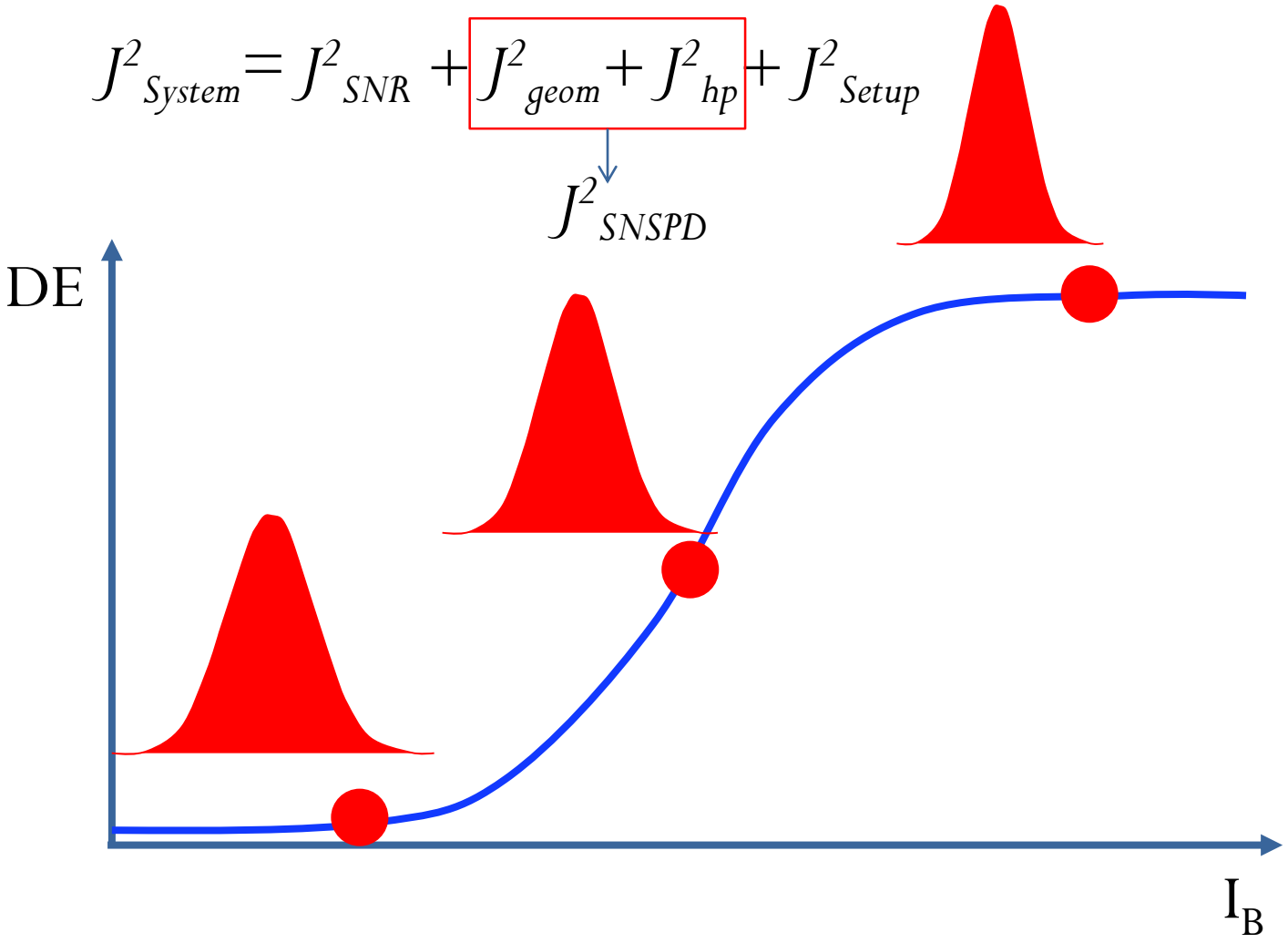

Timing resolution: Jitter vs I_B

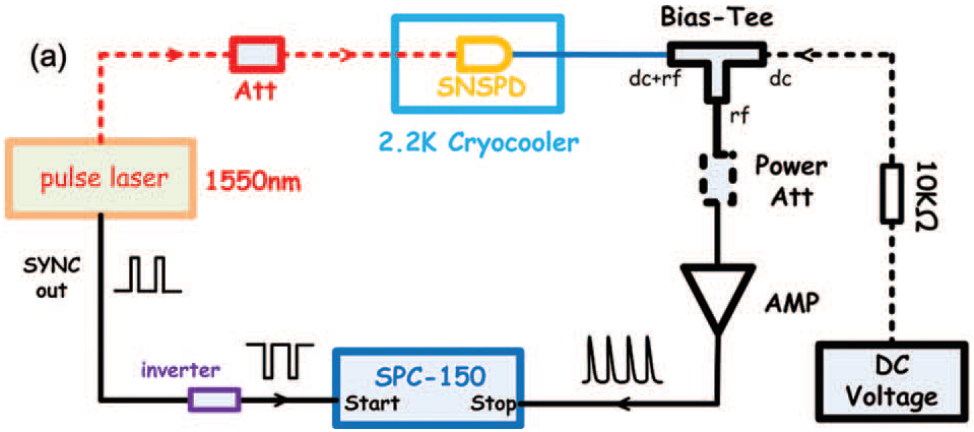

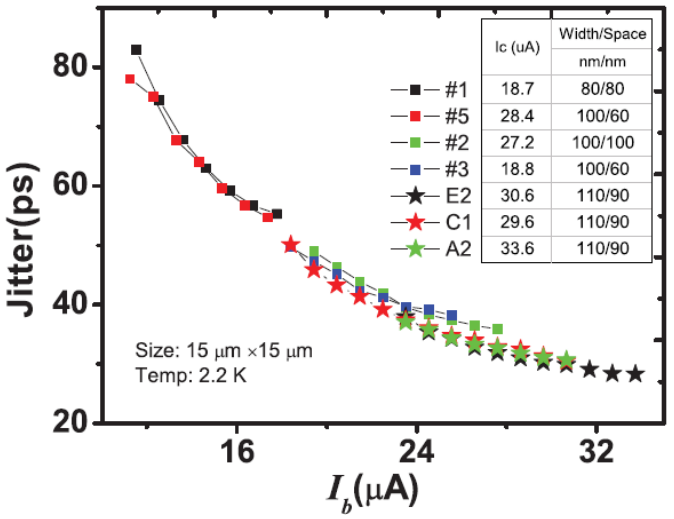

$$j_{system} = \sqrt{j_{SNSPD}^2 + j_{laser}^2 + j_{SYNC}^2 + j_{SPC}^2},$$

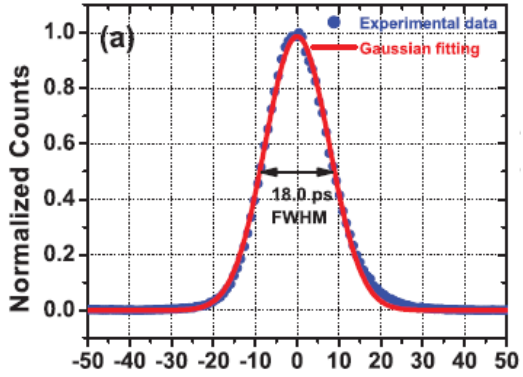

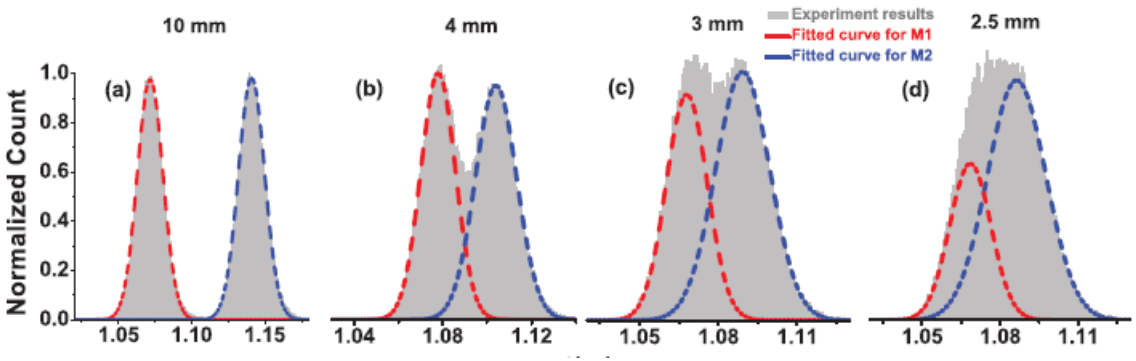

L. You et al., AIP Advances (2013)

λ=1550 nm, LiDAR, time of flight TOF WD ~115 m with a depth resolution of 3 mm.

CNR IFN Istituto di Fotonica e Nanotecnologie

Single photon emitter characterization

Source 1:

CW or Pulsed Laser

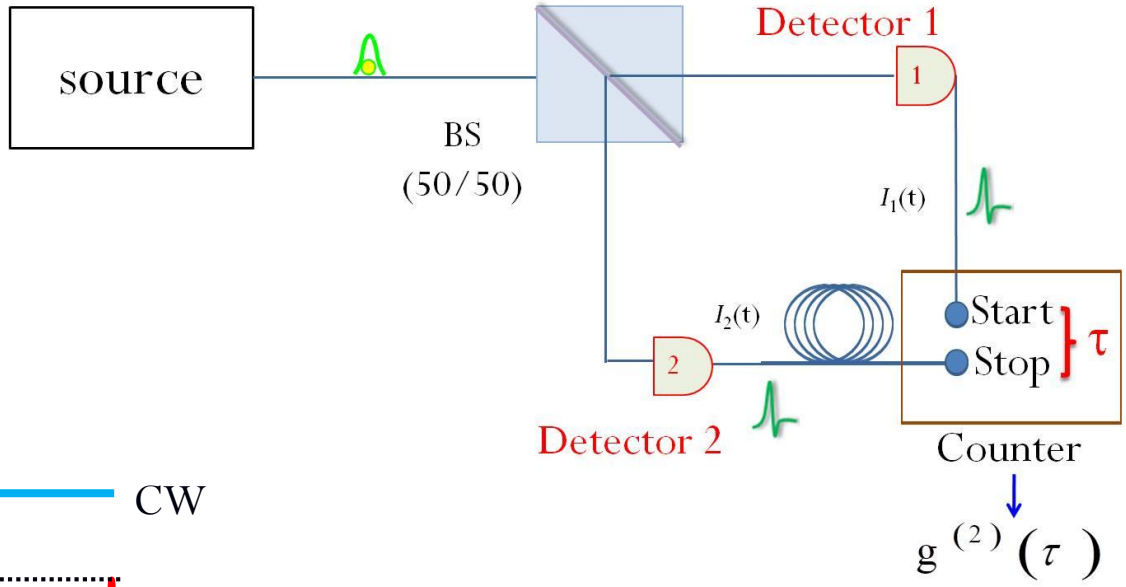

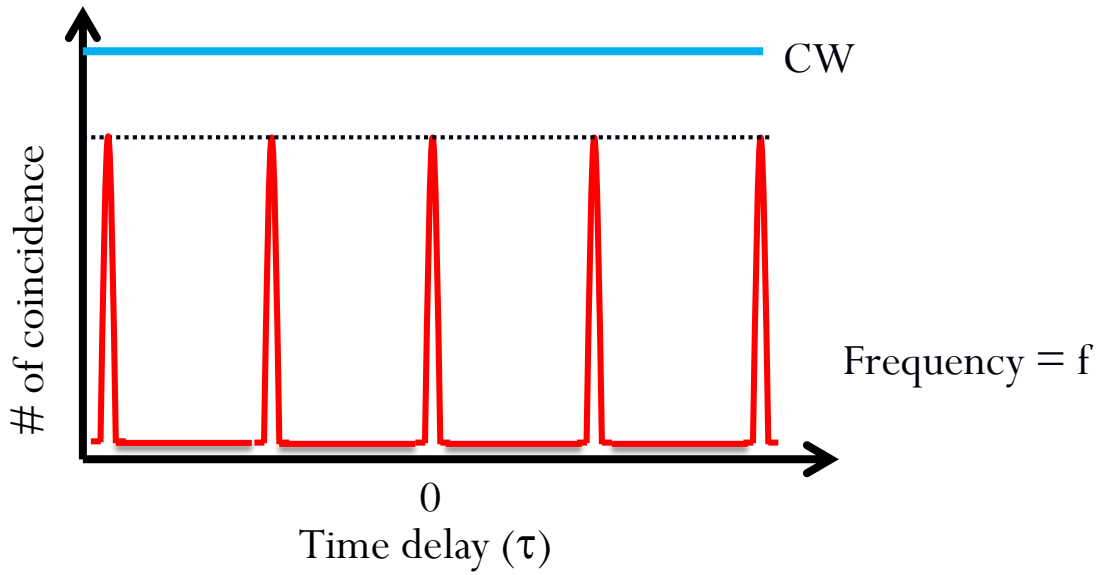

CNR IFN Istituto di Fotonica e Nanotecnologie

Single photon emitter characterization

Source 2:

Quantum emitter of single photons

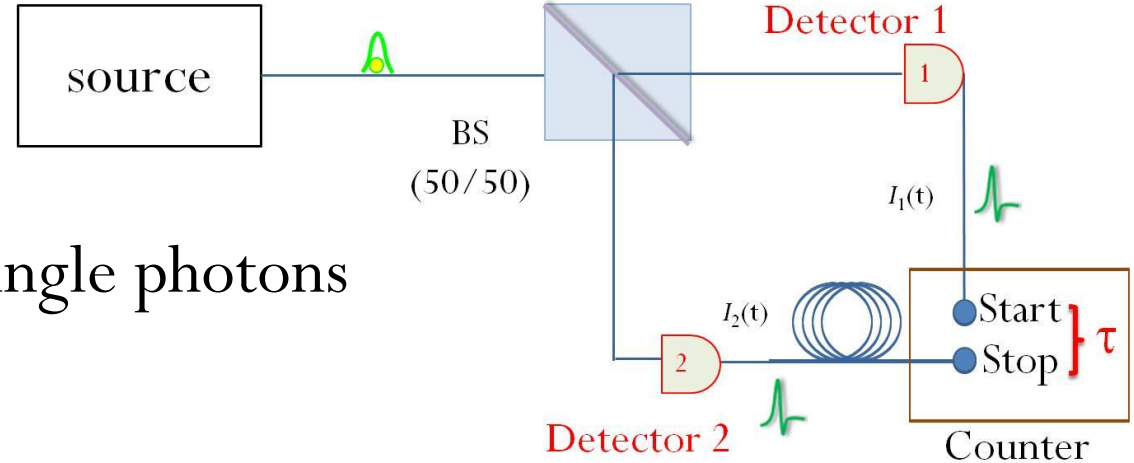

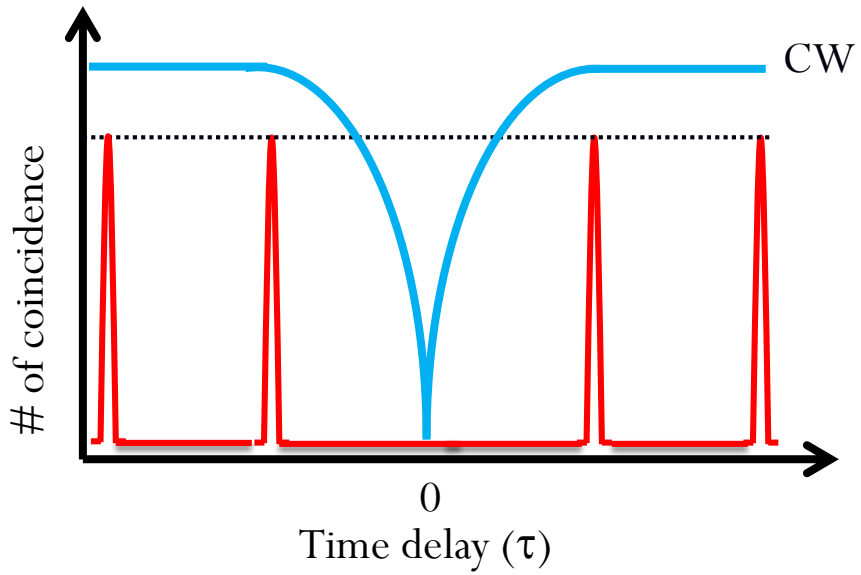

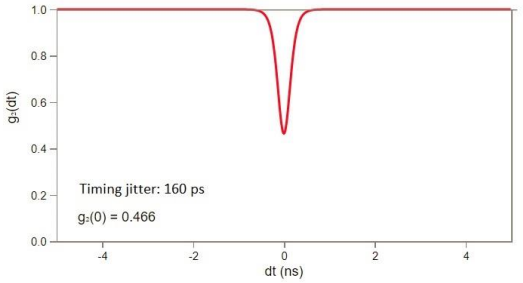

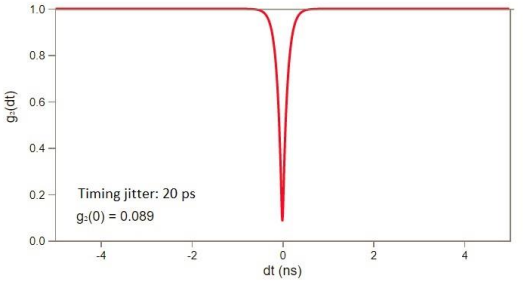

Timing resolution: Jitter

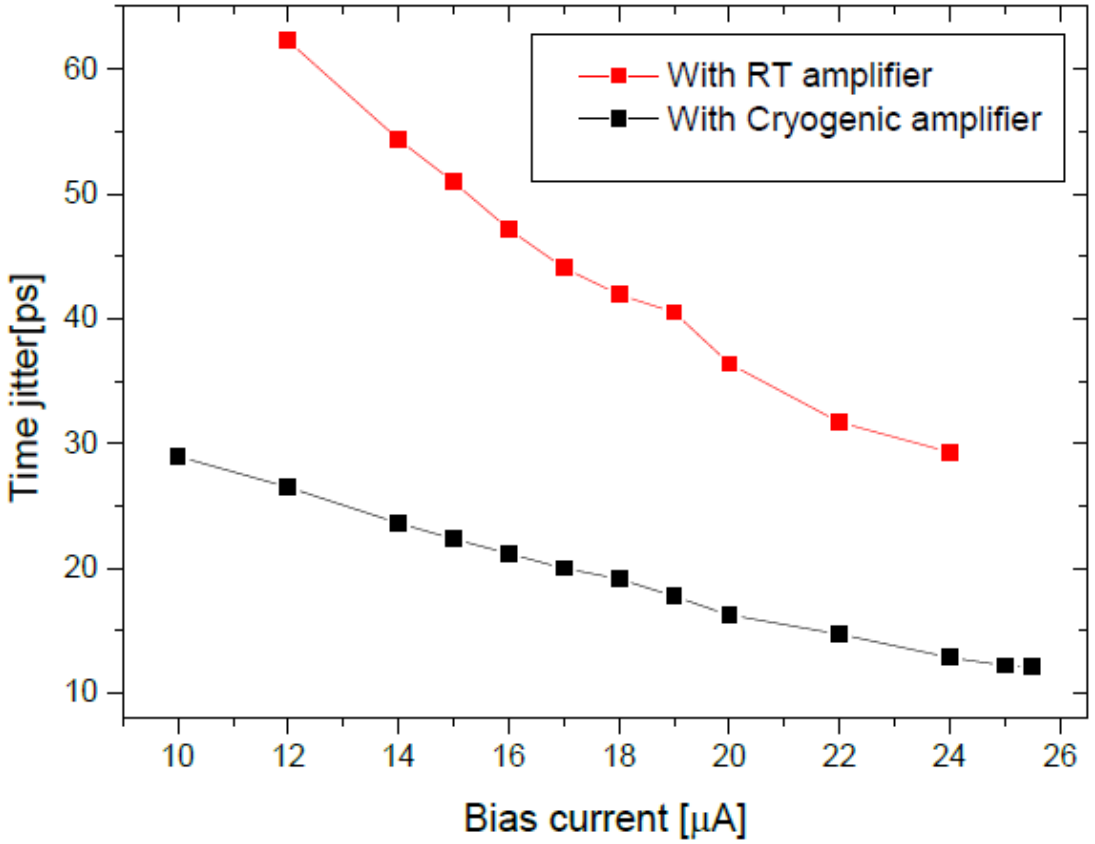

I. Zadeh et al., arXiv (2018)

Adding Detection Functionality to PICs

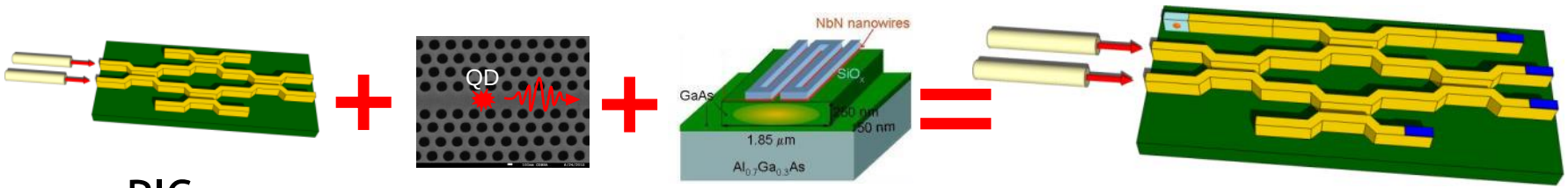

PIC

single photon sources

SNSPDs

GaAs substrate

Conventional approach

CNR IFN Istituto di Fotonica e Nanotecnologie

Waveguide Single Photon Detectors: GaAs

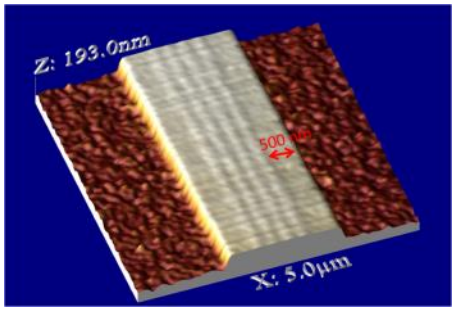

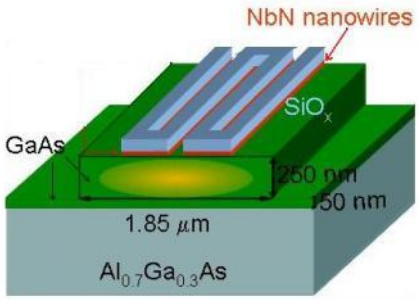

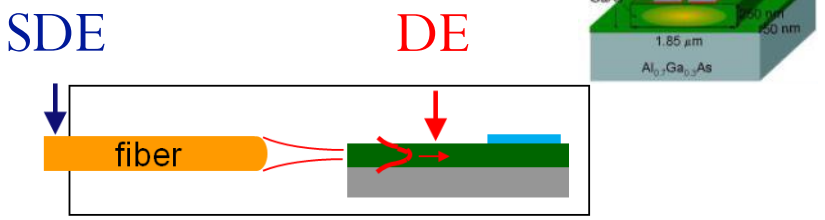

End fire coupling

J. P. Sprengers, Gaggero et al APL (2011)

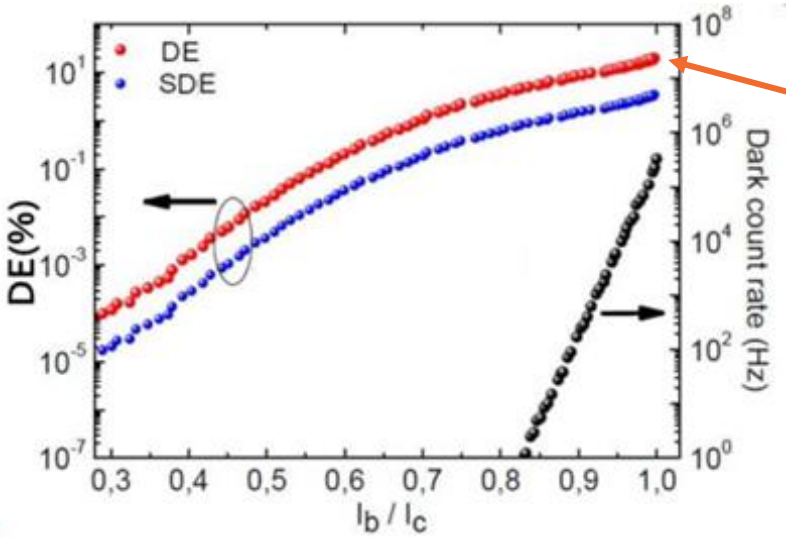

DE = 20 %
SDE = 3.4 %
η_c = 17 %

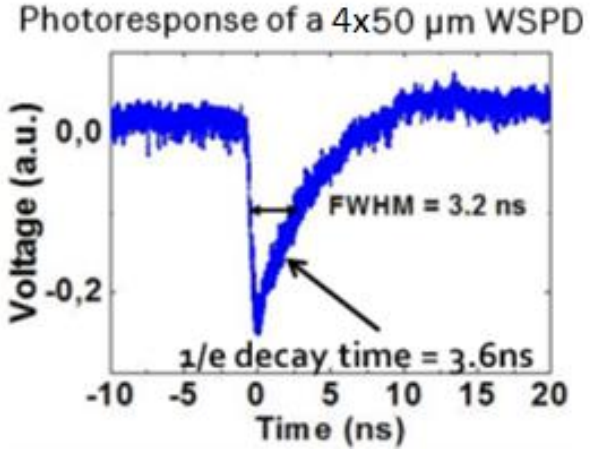

η_c is low, but the goal is to integrate either sources and detectors in the PICs

Coll. TUE CNR-IFN

CNR IFN Istituto di Fotonica e Nanotecnologie

Waveguide Single Photon Detectors: SOI

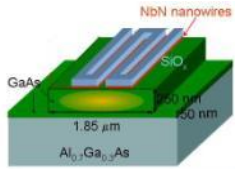

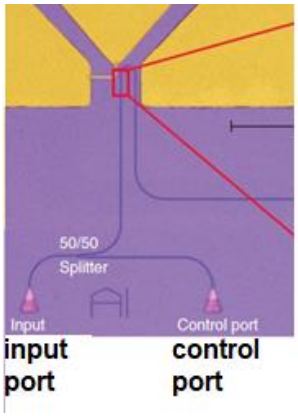

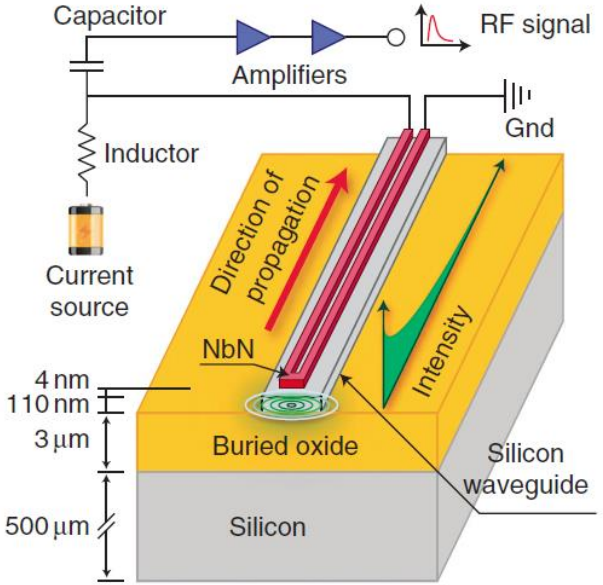

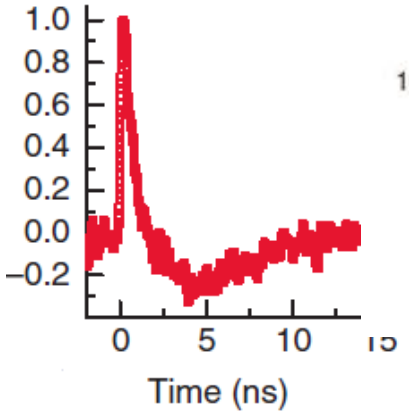

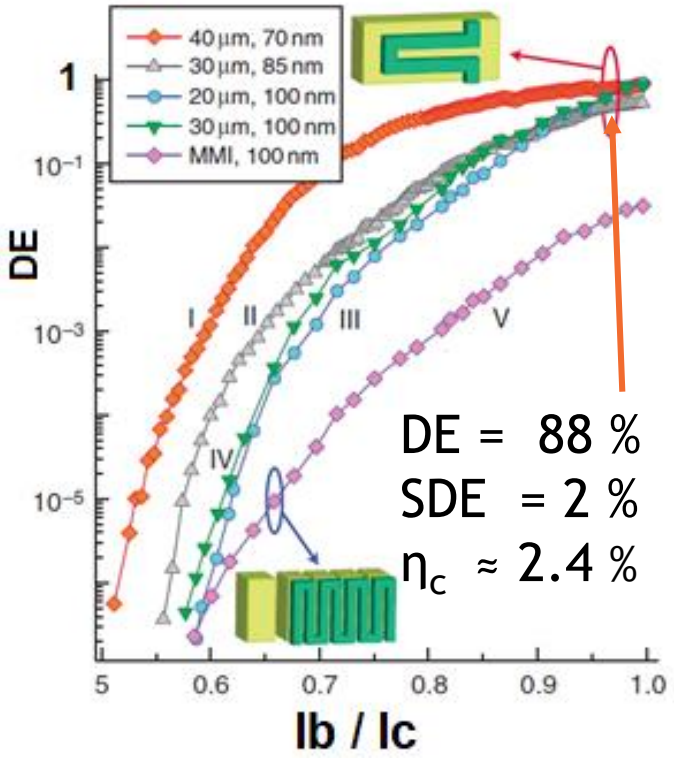

SOI vs GaAs

- Higher index contrast
- Higher NbN deposition temperature

Pernice et al., Nat Comm (2012)

CNR IFN Istituto di Fotonica e Nanotecnologie

After these first succesful integrations of WSPDs on GaAs and SOI platforms, this approach has been followed also on SiN, Diamond and (work is in progress) on AlN and SiC and other materials suitable for integrated photonics.

Photon Number Resolution

Strongly non-linear response!

Linear response vs # of detected photons

photon number resolving detectors (PNRDs):

- have the sensitivity at level of single photon
- Have an output proportional to the # of incident photons.

Photon Number Resolving detectors

- Photon number resolution achieved using the concept of spatial multiplexing.
- The area of the detector is divided in pixels, i.e. smaller meanders with equal resistors in parallel.
- Pixels are connected in series

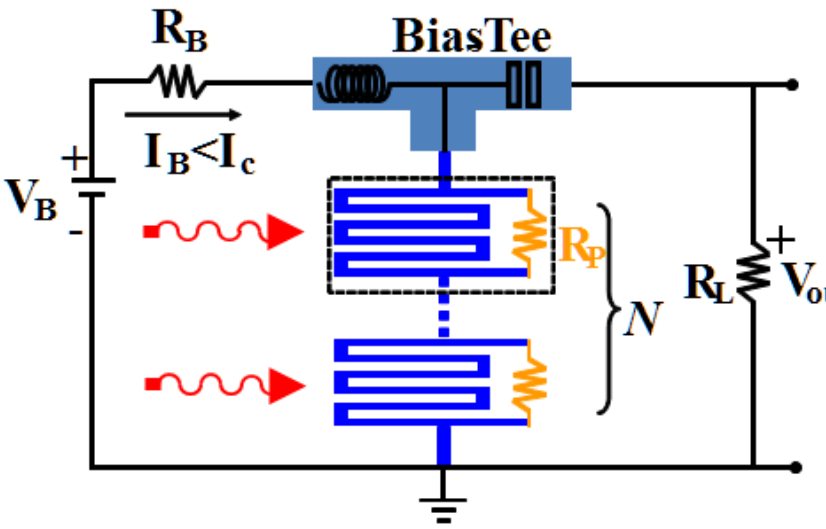

Series nanowire detector

Jahanmirinejad et al Opt. Exp. (2012)

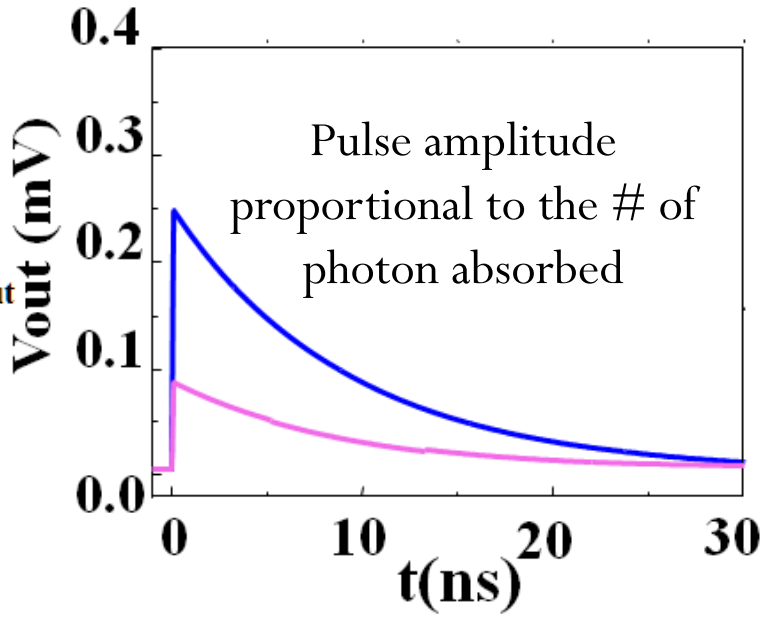

4-Pixels Waveguide PNRD: GaAs

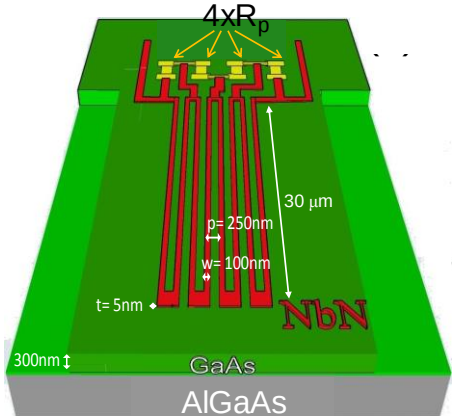

Sahin, Gaggero et al APL (2013)

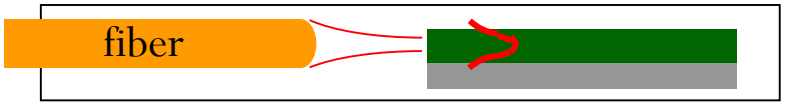

The nanowires are distinct detecting elements sensing different parts of the same waveguide mode

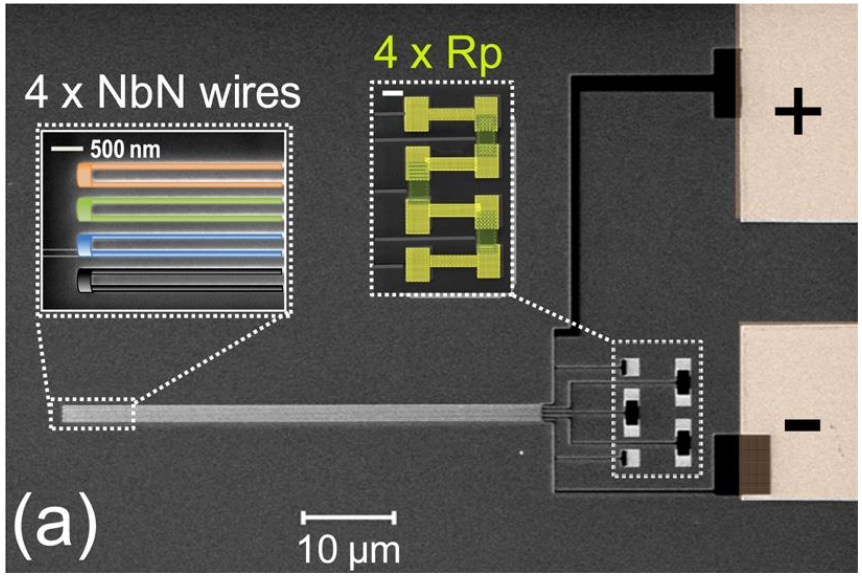

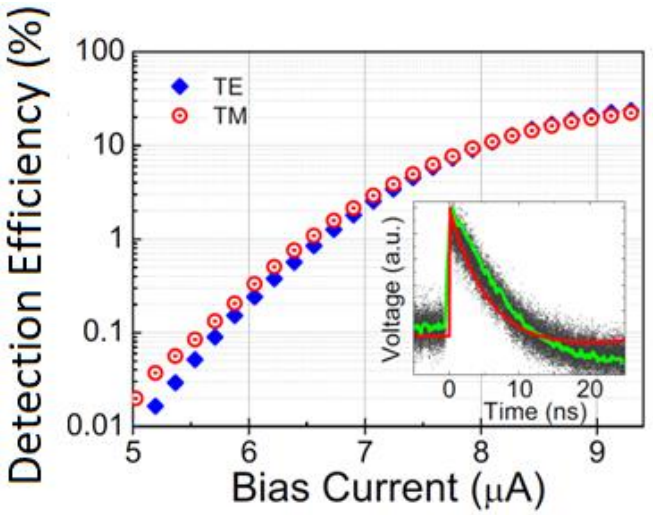

$DE_{(TM)} = 22\%$

$DE_{(TE)} = 24\%$

$\lambda = 1300nm$;

$T < 4\ K$

Coll. TUE CNR-IFN

CNR IFN Istituto di Fotonica e Nanotecnologie

4-Pixels Waveguide PNRD: GaAs

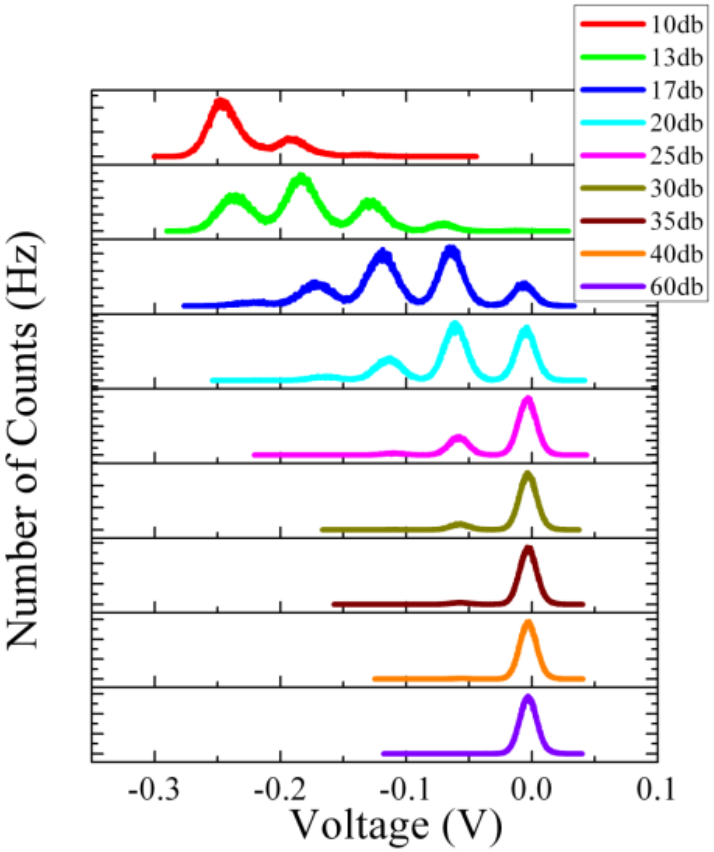

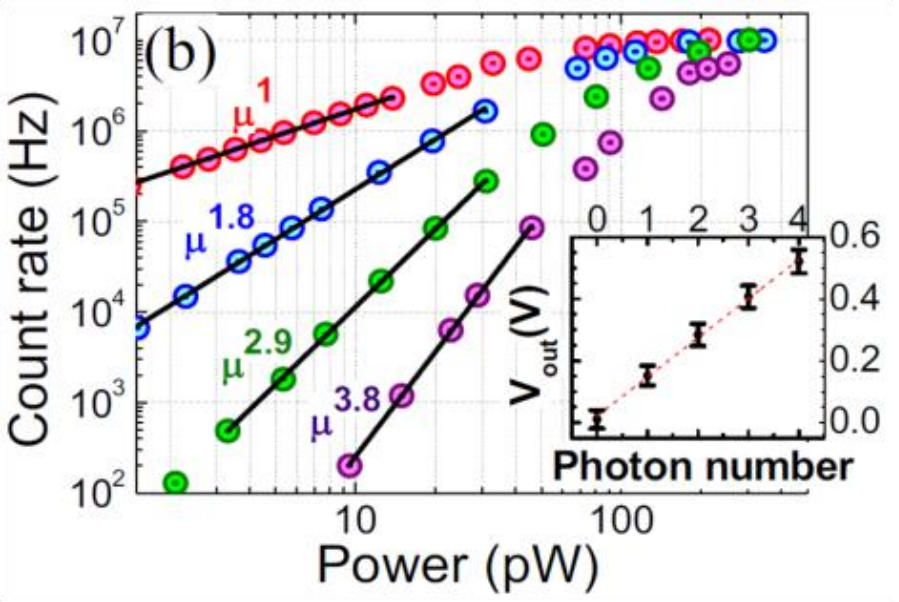

$P(n, \mu) \propto \mu^n$, for a Poissonian source in the regime, where detected average photon number $\mu << 1$, as shown by the fits.

Readout

Deep Space Communications

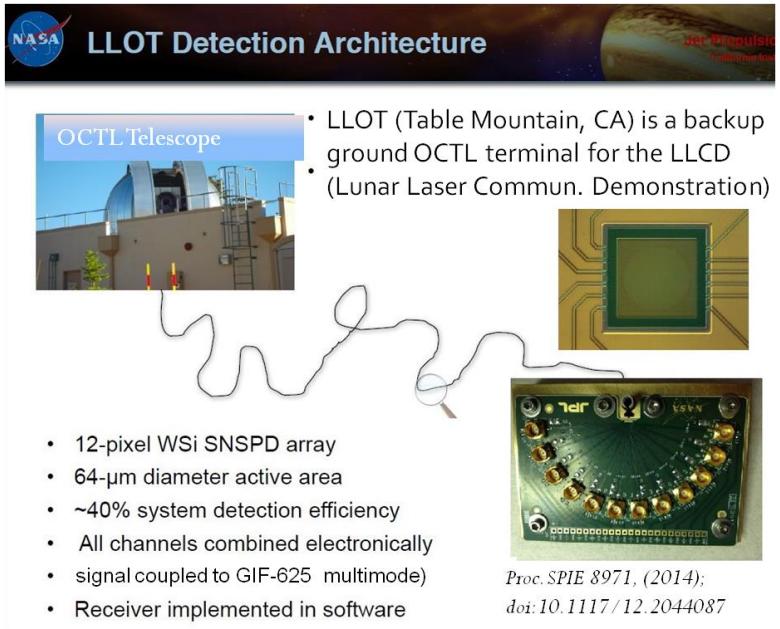

Proc. SPIE 8971, (2014); doi: 10.1117/12.2044087

Integrated Photonic Circuits.

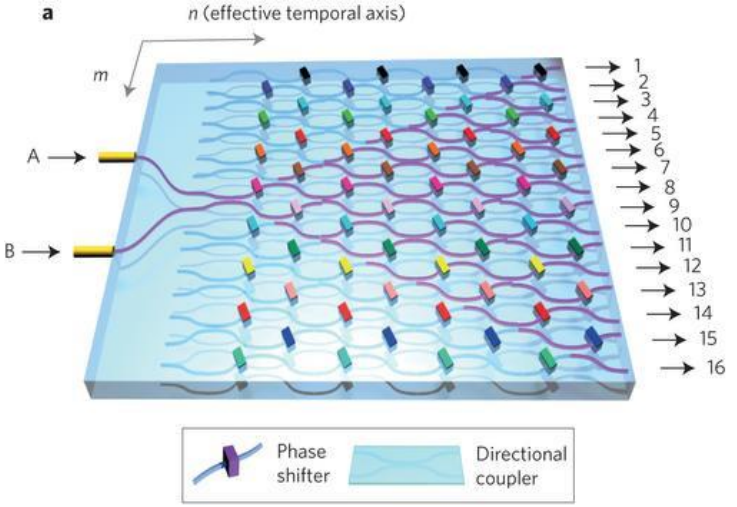

Crespi et al., Nature Photonics 7, 322 (2013)

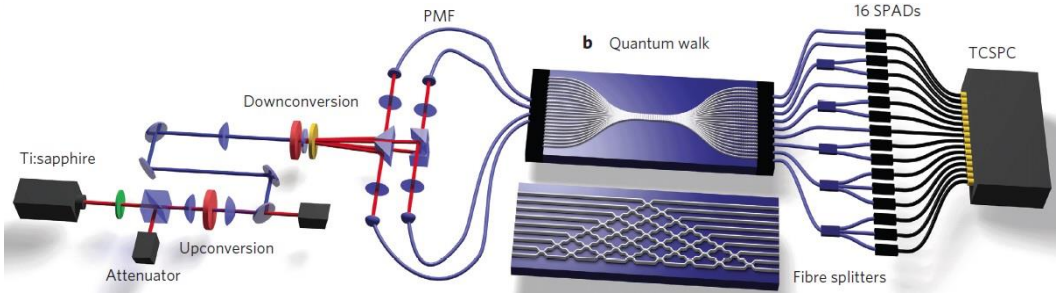

Carolan et al., Nature Photonics 8, 612 (2014)

CNR IFN Istituto di Fotonica e Nanotecnologie

Readout

Verma et al.; *Appl. Phys. Lett.*, 104 (2014)

Readout circuit:
NxN detectors
2N coaxial cables

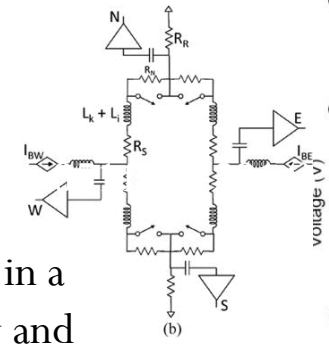

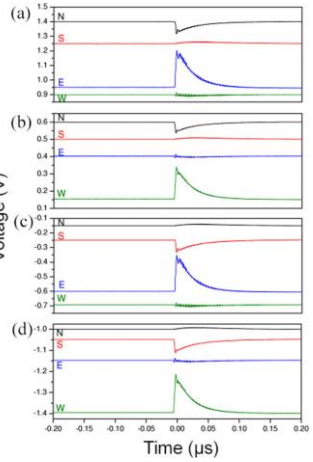

Position is encoded in a combination of row and column pulses

NIST

2 coaxial cables: frequency division multiplexing scheme (usually used for KIDs)

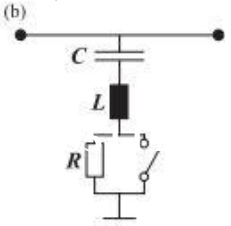

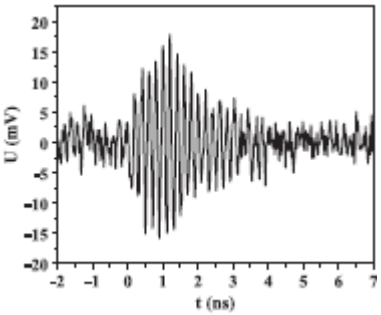

Karlsruher Institut für Technologie

Doerner et al., Ieee Trans. App. Super., 26, (2016)

Zhu et al., nat. Nanotech., 13, 596,(2018)

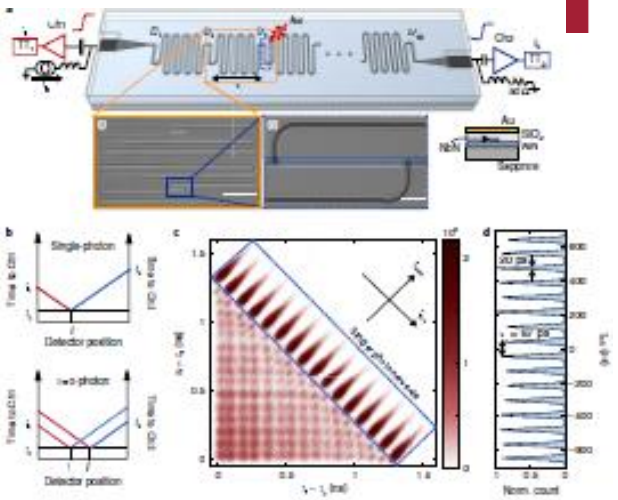

Low temperature SFQ readout electronic

NICT

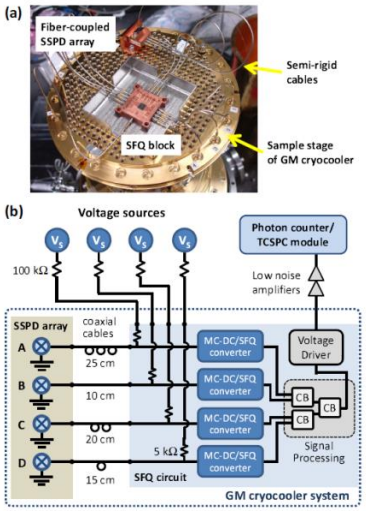

Yamashita et al., Opt. Lett., 37, 2982 (2012)

CNR IFN Istituto di Fotonica e Nanotecnologie

Readout

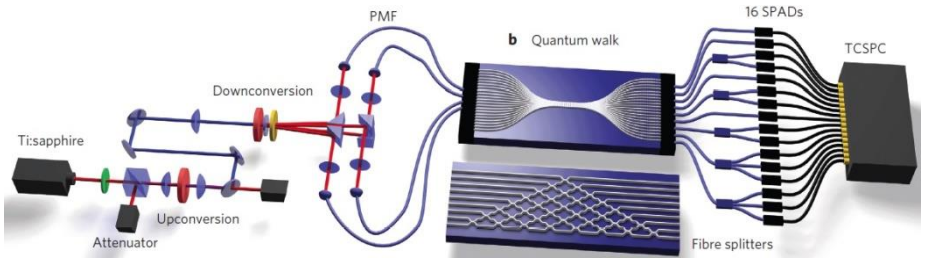

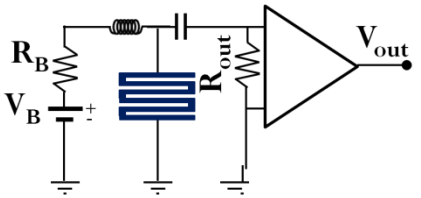

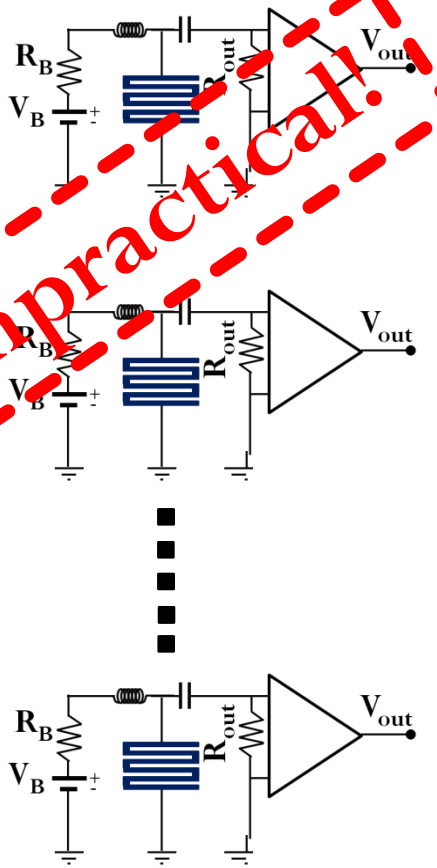

INTEGRATED PHOTONIC CIRCUITS.

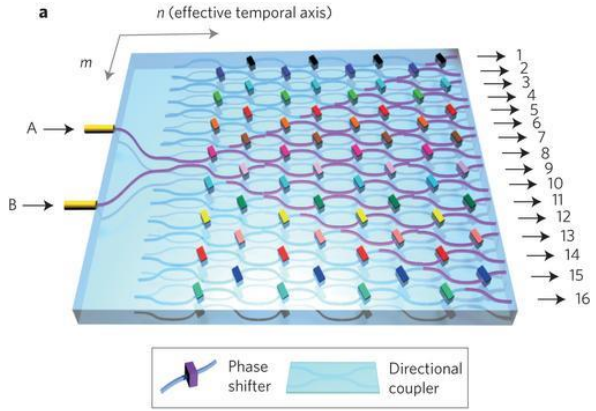

CNR IFN
Istituto di Fotonica e Nanotecnologie

Amplitude Multiplexing

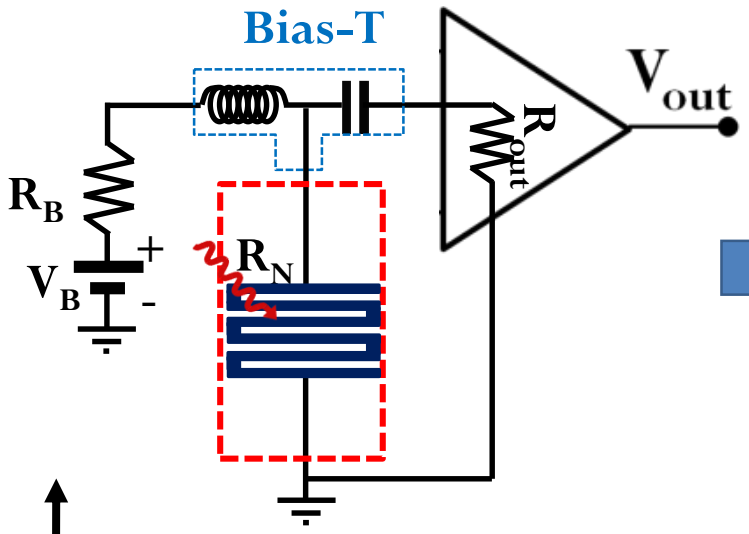

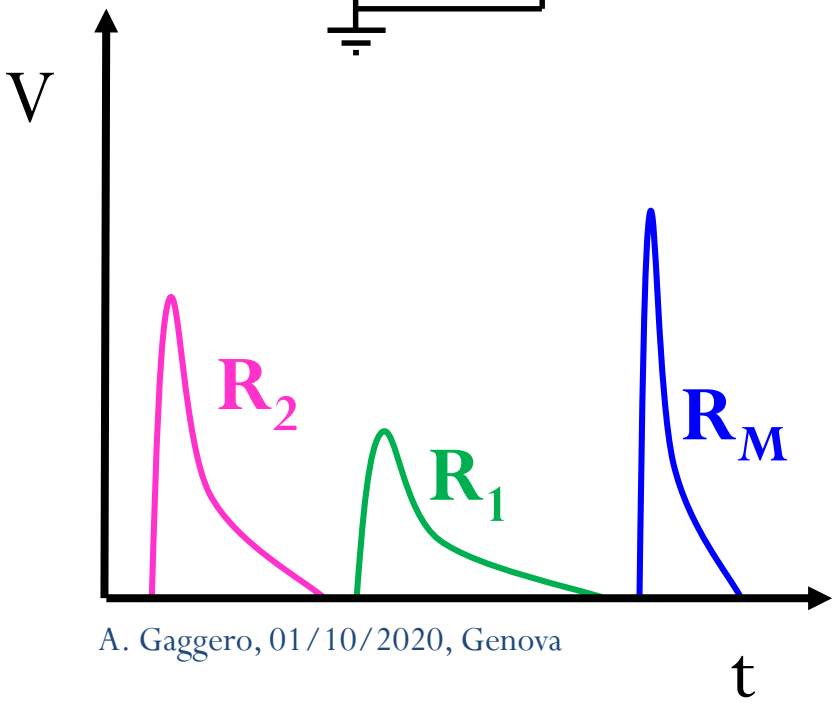

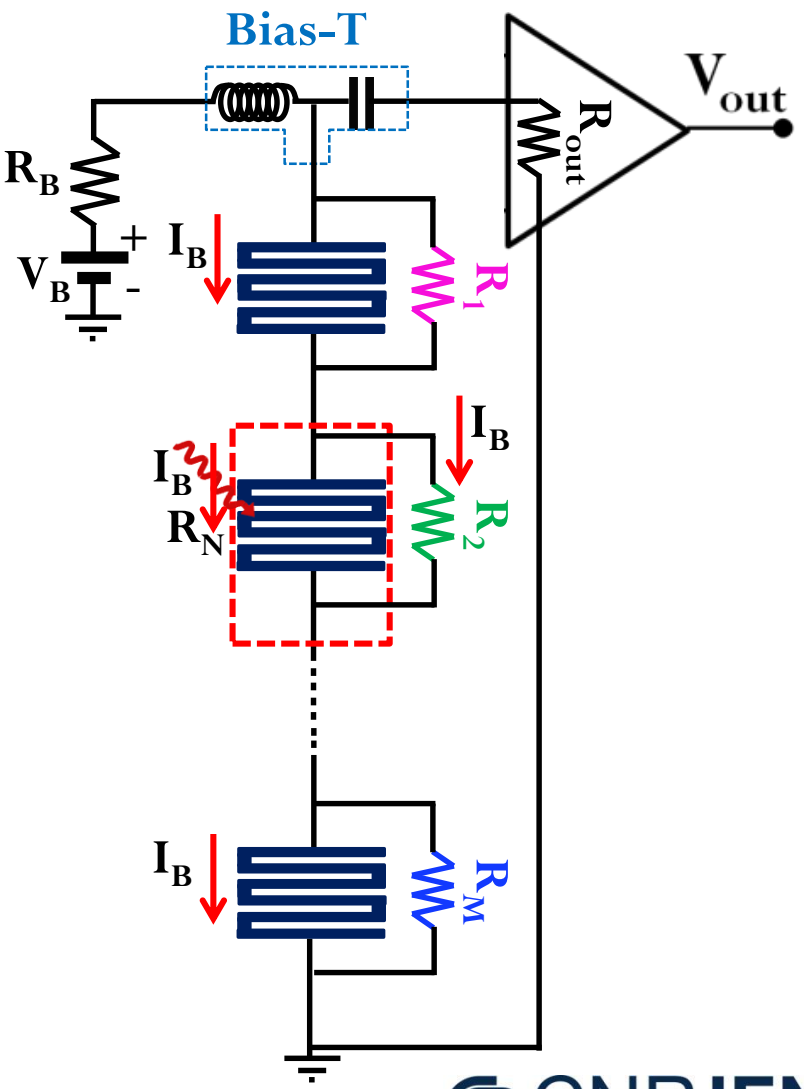

CNR IFN
Istituto di Fotonica e Nanotecnologie

Integrated array

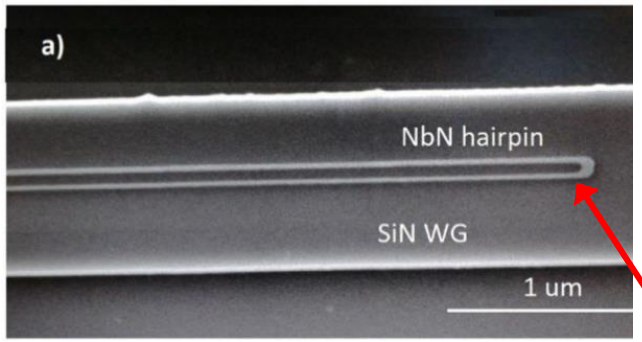

6 nm thick, 80nm wide NbN nwrs
350 nm thick and 1.9 μm wide S_3N_4 ridge Wg

Grating Simulated CE=35% @1530nm @ 300K
measured CE=10% @1550nm @ 300K

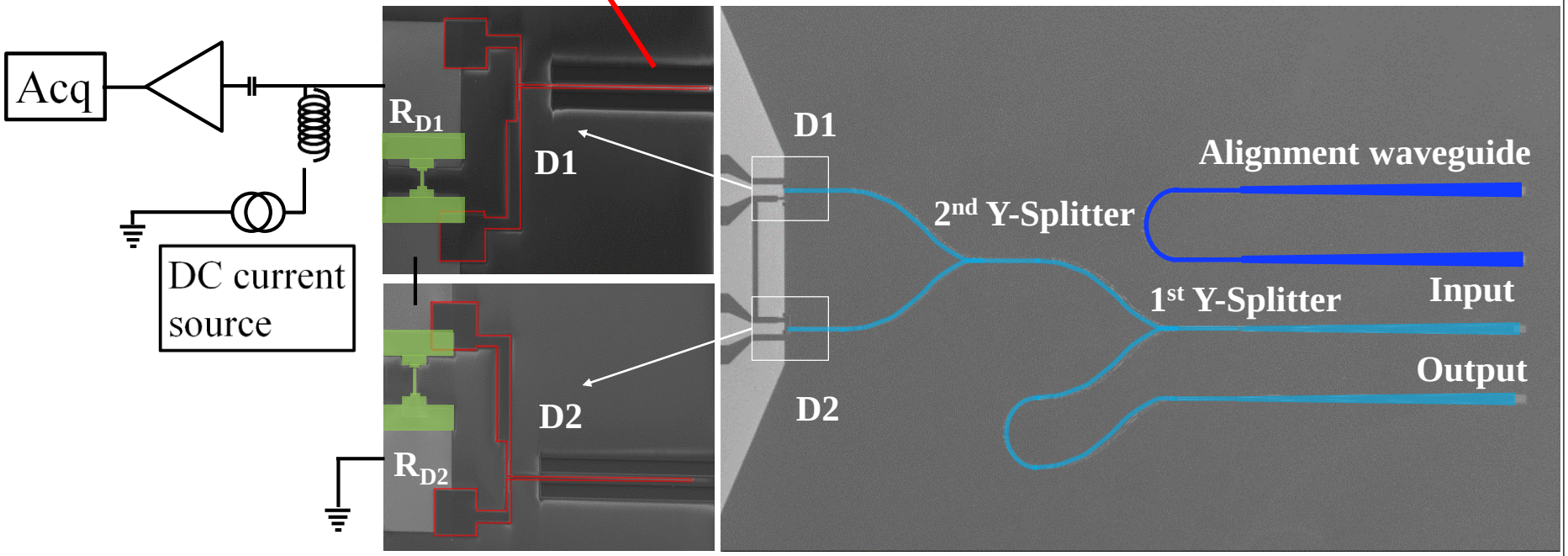

Gaggero et al. Optica (2019)

Set-up

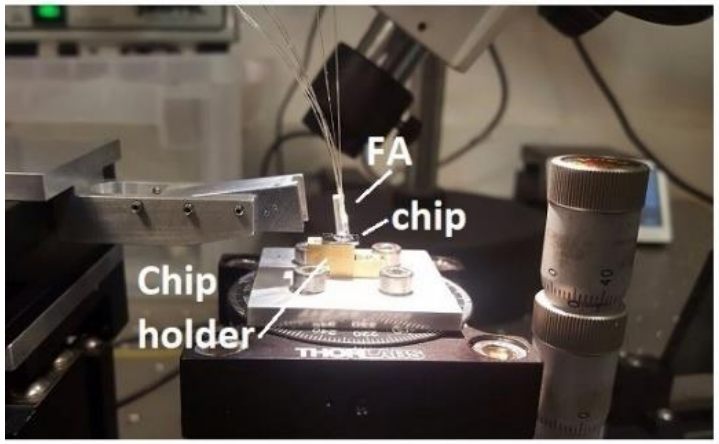

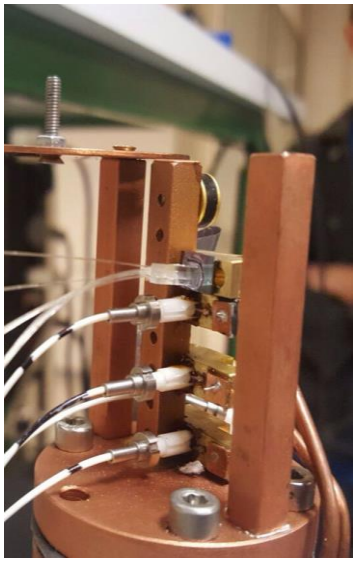

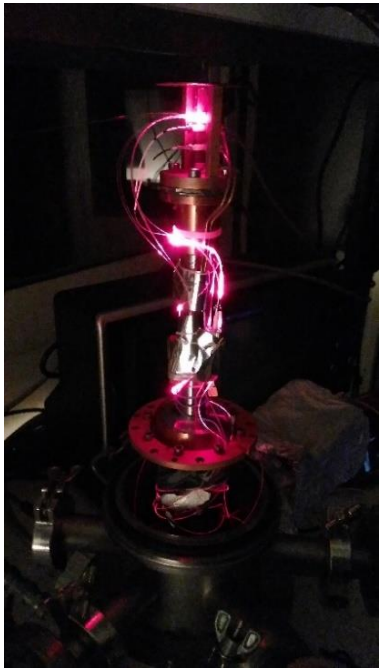

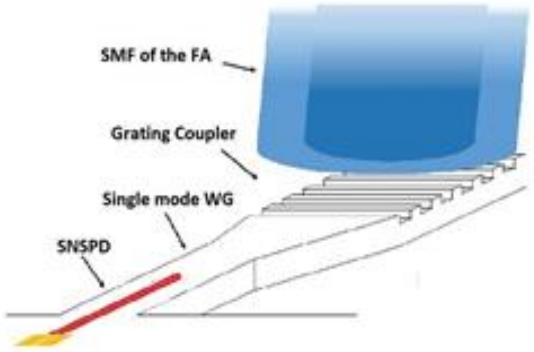

DC

Bias T

Rf

Rf Amplifiers

Power meter

Bias source

DC + Rf

counter 350 MHz

99 %

1 %

λ =1.55 μm Cw/pulsed laser

variable attenuator

4GHz oscilloscope

CNR IFN Istituto di Fotonica e Nanotecnologie

Optical Characterization @T<3K

λ= 1550 nm, f= 1MHz, <n> = 0.1
Pulse width 10 ps

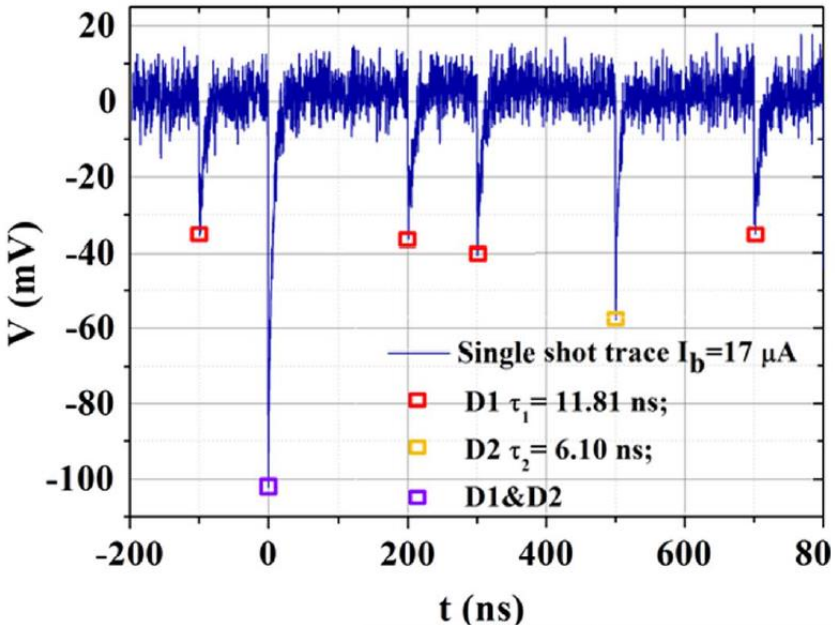

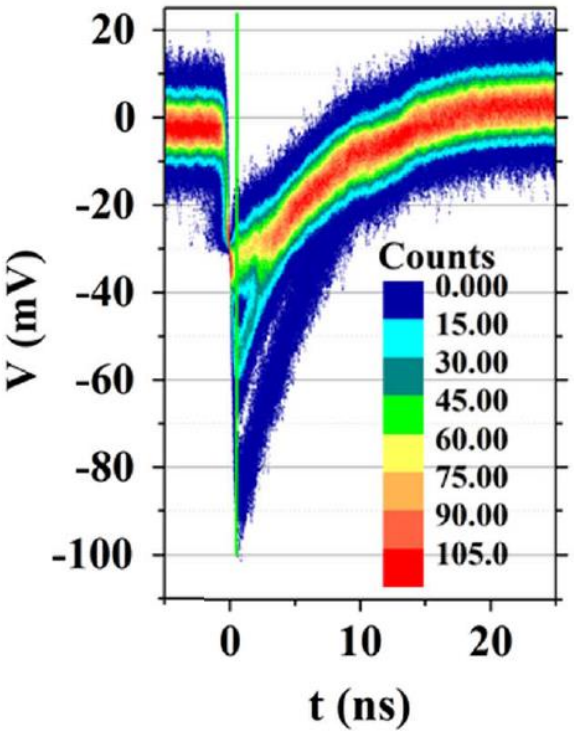

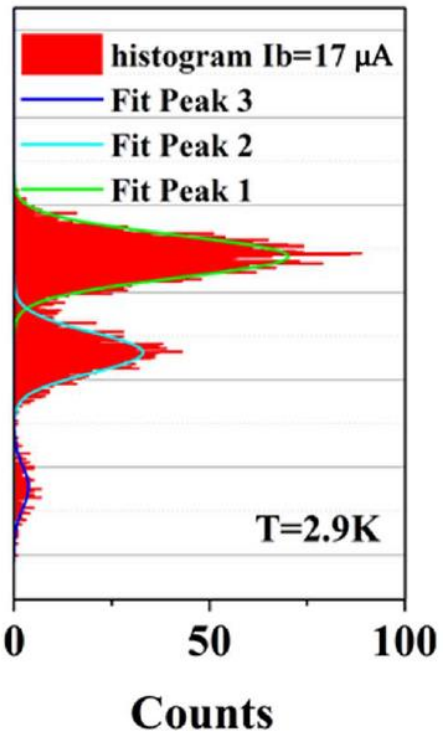

Optical Characterization @T<3K

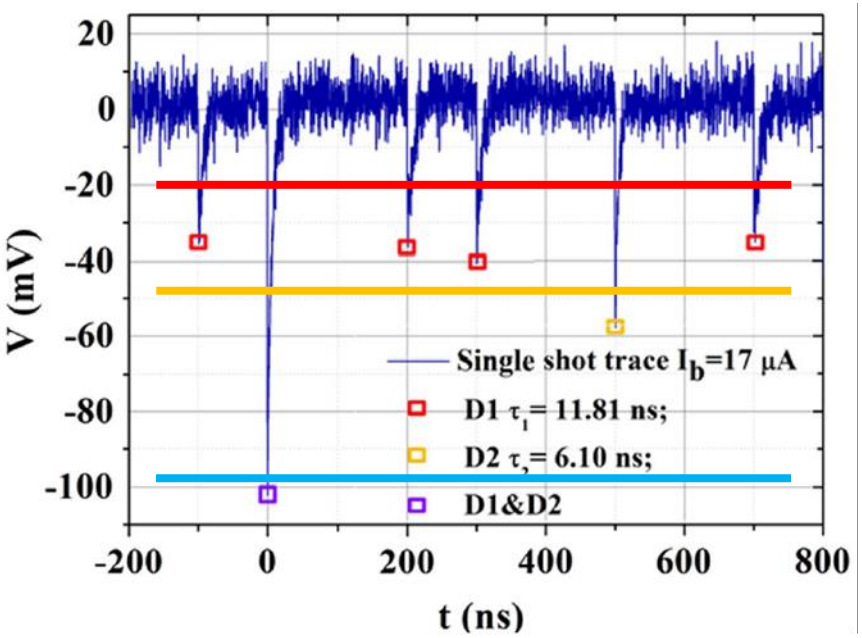

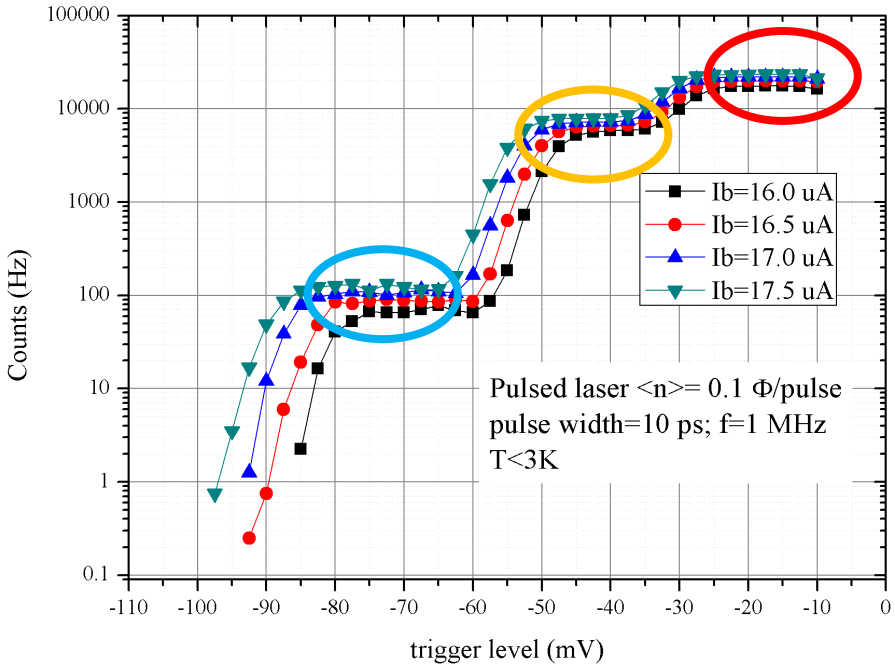

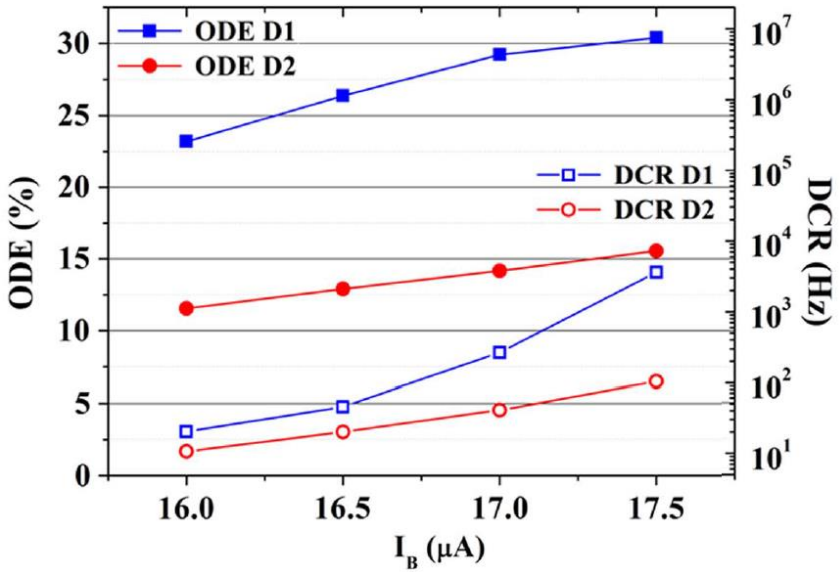

λ= 1550 nm, f= 1MHz, <n> = 0.1
Pulse width 10 ps

ODE_{d1}= 30.4 % @ 4 kHz DCR
ODE_{d2}= 15.6 % @ 100 Hz DCR

CNR IFN Istituto di Fotonica e Nanotecnologie

Scalability

Gain~ 49 dB @ 500MHz

$V_\sigma = 3.7$ mV

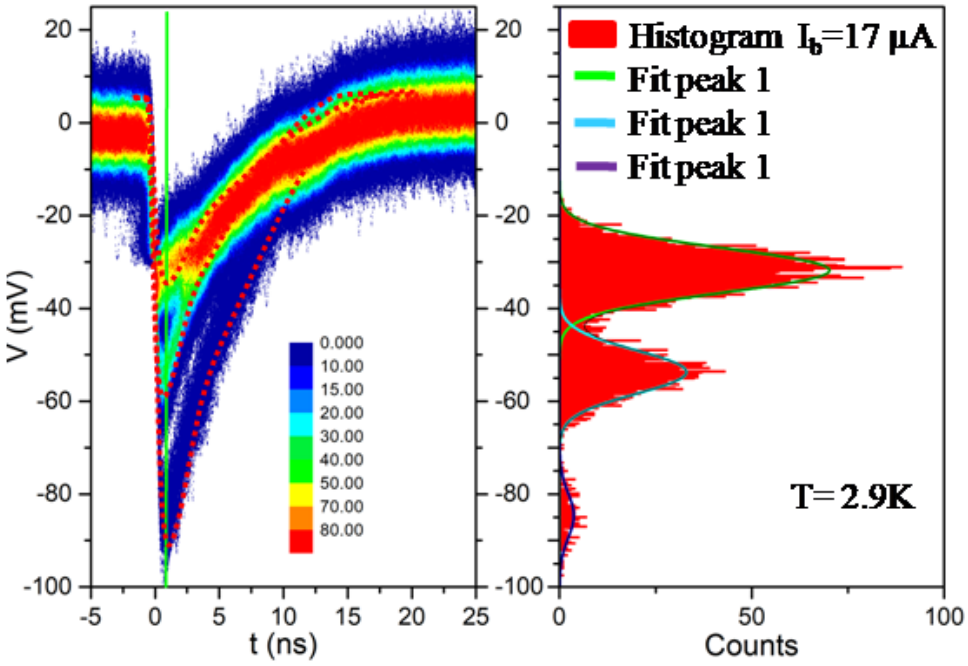

$I_B = 17.0\ \mu A \Rightarrow \Delta R_{2\sigma} = V_{2\sigma} / I_B = 1.6\ \Omega$

$\Delta R_{6\sigma} = V_{6\sigma} / I_B = 4.7\ \Omega$

$V_{th} = (4k_B BT50\Omega)^{1/2} = 20.3\ \mu V \Rightarrow \Delta R_{th} = 1.2\ \Omega$

$Ch_i = R_M / \Delta R_i$

R_{in} (Ohm)	T (K)	B (MHz)	ΔR_{th} (Ohm)	$\Delta R_{2\sigma}$ (Ohm)	$\Delta R_{6\sigma}$ (Ohm)	R_M (Ohm)	$Ch_{2\sigma}$	$Ch_{6\sigma}$
50	300	0.1-500	1.2	1.6	4.7	50	30	10

Prospects: Scalability

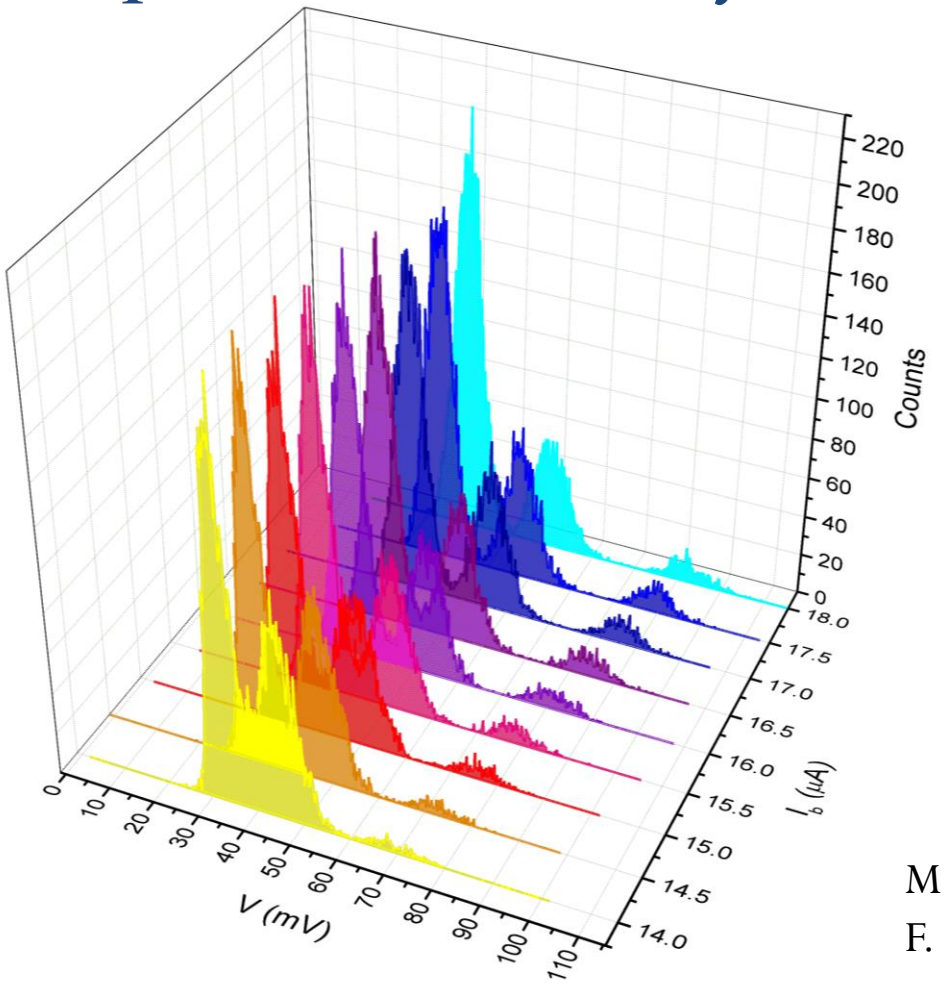

Gain~ 49 dB @ 500MHz

$V_{th} = (4k_B BT50\Omega)^{1/2}$

M Ejrnaes et al. *Appl. Phys. Lett.*, 91 (2007)
F. Marsili et al., Nano Lett. 11 (2011)

CNR IFN Istituto di Fotonica e Nanotecnologie

Prospects: Cryogenic Amplifier

$$V_{th} = (4k_B B T R_{in})^{1/2}$$

NF @ 20 K: < 0.11 dB, from .0001 to 1.5 GHz

NF @ 300K <1.5 dB from .0001 to 1.5 GHz

www.cosmicmicrowavetechnology.com/citlf1

R_{in} (Ohm)	T (K)	B (MHz)	R_{th} (Ohm)	$\Delta R_{2\sigma}$ (Ohm)	$\Delta R_{6\sigma}$ (Ohm)	R_M (Ohm)	$Ch_{2\sigma}$	$Ch_{6\sigma}$
50	300	0.1-500	1.2	1.6	4.7	50	30	10
50	20	0.1-500	0.31	0.4	1.2	50	121	41

Thank you for the attention!

CNR IFN
Istituto di Fotonica e Nanotecnologie